CHAPTER IV
EFFECTS OF DYNAMIC VULCANIZATION, CURING AGENT, RUBBER CONTENT AND POLY(LACTIC ACID) ON PROPERTIES OF ENR/PVDF BLENDS

4.1 Abstract

This study is purposed to develop a thermoplastic vulcanizate (TPV) via dynamic vulcanization made of ENR and poly(vinylidene difluoride) (PVDF). The effects of dynamic vulcanization, contents of ENR and curing agent (DBPH) and addition of PLA on mechanical and oil swelling properties were studied to observe suitable formula for making TPV blends which can be able to use in automotive and chemical industries. Rubber parts were mixed at room temperature by using two roll mill, fed in twin screw extruder with thermoplastic parts to allow dynamic vulcanization and then compressed in compression molding. This research was emphasized on the contents of ENR (50, 60 and 70 wt%), PVDF, DBPH (3, 5 and 7 phr) and the addition of PLA at fixed 10 wt% that affect on the properties of the dynamic blends in comparison to the ternary ones (the blends among ENR, PVDF and PLA). The results showed that the dynamic vulcanization and the increase in thermoplastic and DBPH contents have enhanced the mechanical properties (tensile and tear strength and hardness) and oil swelling resistance.

4.2 Introduction

The production of rubber parts become a big market because it have high consumption in fuel and chemical transmission line in automotive and chemical industries such as, gasket, suspension bush, oil tank plug and drain pipe. The rubbers used for special applications like these have prominent properties for example, flexibility, thermal resistance, chemical and oil resistance, compressibility, impact resistance, and friction resistance.

Dynamic vulcanization is the vulcanization process of an elastomer during its melt mixing with a thermoplastic, which results in a new class of materials called

thermoplastic vulcanizates (TPV). The initial stage of vulcanization show co-continuous morphology, then apply any torque or shear rate, rubber phases are going to be separated gradually until the final stage which exist the fine dispersed morphology of rubber particles within thermoplastic matrix.

Fluoroelastomer (FKM) is well known for an excellent thermal, oil and chemical resistances but the price of FKM is still high therefore the dynamically vulcanized blends of epoxidized natural rubber (ENR) and poly(vinylidene fluoride) (PVDF) have been recognized as TPV materials which are promising candidates to be able to use instead of synthetic rubber. Supri and H. Ismail [1] reported dynamically vulcanized blends of poly(vinyl chloride)/acrylonitrile butadiene rubber (PVC/NBR) gave better results than binary blends in terms of mechanical properties, swelling resistance, thermal stability and interaction between PVC and NBR. The results of Yamoun C. [2] suggested that DBPH peroxide curing system worked better as a curing agent for dynamic vulcanization of natural rubber/fluoroelastomer/high-density polyethylene (NR/FKM/HDPE) than DCP sulfur system on mechanical properties, degree of cross-linking, compatibility and morphology. Furthermore, Phothiphon K. [3] was found that increasing DBPH content in natural rubber/poly(vinylidene fluoride)/ poly(3-hydroxybutyrate-co-3-hydroxyvalerate) (NR/PVDF/PHBV) blends via dynamic vulcanization resulted to better tensile and tear strength and oil swelling resistance.

In this work, PVDF and PLA used as thermoplastic parts to provide oil and chemical resistant properties and make it more environmental friendly, respectively. ENR used as rubber part to provide the elastomeric properties. This research report the effects of dynamic vulcanization, contents of ENR, PVDF and curing agent and addition of PLA on mechanical properties (tensile and tear strength and hardness), thermal properties (DSC and DMA), curing properties (MDR), oil swelling resistant properties and morphology (SEM) of the blends.

4.3 Experimental section

4.3.1 Materials

The materials used in this study were ENR with 25 % epoxidation, supplied by Muang Mai Guthrie PCL., PVDF (grade Z100), supplied by Asambly Chemicals Company, PLA (grade 2002D), supplied by NatureWorks LLC. The selected additives (Fluka reagent grades) were calcium hydroxide ($Ca(OH)_2$) and 2,5–bis(tert–butylperoxy)–2,5–dimethylhexane (DBPH). Triacetin was supplied by Sigma-Aldrich Co. LLC. Stearic acid and triallyl isocyanurate (TAIC) were purchased from Neo plastomer Co.,Ltd. Gasohol 91, 95, E20 and E85 were supplied by PTT PCL.

4.3.2 Preparation of the blends

4.3.2.1 Preparation of rubber parts

The ENR compounds were prepared for curing characterization by using MDR and DSC. They were blended by using an internal mixer at room temperature with a rotor speed of 50 rpm. The ENR was charged first into the mixing chamber, then stearic acid, $Ca(OH)_2$, TAIC and DBPH were added, respectively. Mixing was then continued until a constant torque was obtained. The total mixing time was 10 minutes. The compound was removed from the mixer and was tested in next steps. The formulations were shown in table 4.1.

Table 4.1 Formulations of ENR blends for curing characterization

Materials	Quantity, phr[a]	Mixing times, min
ENR	100	0 - 2
Stearic acid	0.25	2 - 3
$Ca(OH)_2$	3	3 - 6
TAIC	X/2	6 - 8
DBPH	X	8 - 10

Note: [a]phr is part per hundred part of rubber and X is the varying DBPH content at 3, 5 and 7 phr.

4.3.2.2 Preparation of thermoplastic parts

The thermoplastic parts which contain PVDF, triacetin (5 phr) and PLA, if any, were prepared by melt-mixing in a co-rotating twin screw extruder (LTE20-40 model). In case of adding PLA, the PVDF/PLA blends were mixed at composition of 80/20. The temperature profile from the feed zone to the die is 175, 180, 185, 185, 190, 190, 195, 195, 200, 210 °C. The screw speed was used at 50 rpm. The extrudate was cooled in water bath and then cut into pellet by pelletizer.

4.3.2.3 Preparation of Thermoplastic vulcanizate (TPV)

The formulations of the TPV blends are given in Table 4.2. First step, the rubber parts were prepared at room temperature by using two roll mill (LRM 110 model). The ENR was mixed with stearic acid, $Ca(OH)_2$, TAIC, DBPH and triacetin, respectively. The total mixing time was 45 min. The compound was removed from two roll mill, cut it to be small strips, put thermoplastic blends pellets which obtained from 4.3.2.2 on top of rubber compound surface and fed in twin screw extruder, respectively.

Last step, the TPV was achieved by blending thermoplastic and rubber via twin screw extruder by using temperature profile from the feed zone to die of 185, 188, 188, 178, 180, 182, 185, 188, 190, 190 °C. The screw speed was used at 70 rpm. Then the extrudate was cooled in water bath and then cut into pellets by pelletizer. The TPV blends pellets were compressed in a compression mold (Wabash MPI, V50H–18–CX model, USA). Hot-press procedures involved pre-heating at 190 °C for 5 min, followed by compressing for 5 min at the same temperature with pressure of 20 tons.

4.3.3 Study of curing properties

The curing properties of rubber parts including cure rate index (CRI), cure time (t_{90}), maximum torque and the practical curing temperature in DBPH system were observed by using MDR and DSC before moving to a compression step. For MDR (rheoTECH MD+,Tech pro, A022S), they were tested under operation of constant conditions (0.5 deg arc strain amplitude, rotor size L) at various

temperatures ranging from 180 – 200 °C. For DSC (DSC822E model, Mettler Toledo), the samples were characterized under nitrogen atmosphere with a flow rate of 10 ml/min. All of samples were heated at 180, 190 and 200 °C for 30 minutes in case of isothermal method and were heated from 30 °C to 300 °C with the heating rate of 10 °C/min in case of non-isothermal method.

Table 4.2 Formulations of ENR/PVDF/PLA blends

Materials	Blends (wt %)					
	I	II	III	IV	V	VI
ENR	50	60	70	50	60	70
PVDF	40	30	20	50	40	30
PLA	10	10	10	-	-	-
DBPH [a]	X	3	3	X	3	3
TAIC [a]	X/2	1.5	1.5	X/2	1.5	1.5
Stearic acid [a]	0.25	0.25	0.25	0.25	0.25	0.25
$Ca(OH)_2$ [a]	3	3	3	3	3	3
Triacetin [a]	2.5	2.5	2.5	2.5	2.5	2.5
Triacetin [b]	2.5	2.5	2.5	2.5	2.5	2.5

Note: X is the varying DBPH content at 3, 5 and 7 phr, [a] At phr of rubber and [b] At php of plastic. A similar ternary blends of ENR/PVDF with PLA were prepared but without the addition of DBPH, TAIC, Stearic acid and $Ca(OH)_2$.

4.3.4 Study of rheological properties

The viscosity of ENR, NBR, PVDF and PVDF/PLA blends were measured by using rheometer (Ceast 5000 model) at 180, 185, 188 and 190 °C. The L/D ratio of used die was 20/1.The shear rates were determined from 40 to 6,000 (1/s).

4.3.5 Study of thermal properties of TPV blends after twin screw extruder

The thermal properties of TPV blends obtained from twin screw extruder were analyzed using DSC (DSC822E model, Mettler Toledo) and compared with thermograms of PVDF and PVDF/PLA blend. The samples were tested under nitrogen atmosphere with a flow rate of 10 ml/min and heated from 30 °C to 200 °C with the heating rate of 10 °C/min and held for 3 minutes to delete thermal history. Then, they were cooled down to 30 °C and re-heated again to 200 °C at the same heating rate. The melting temperature and cold crystallization temperature were obtained from DSC thermograms. The relative percent crystallinity of PVDF and PVDF/PLA blends at the composition of 80/20; X_{BLEND} (%) were calculated according to the equation 4.1, 4.2 and 4.3, respectively. The TPV with 10 % of PLA at the rubber/thermoplastic composition of 50:50 ratio was calculated according to the equation 4.4:

$$X_{PVDF}(\%) = \frac{\Delta H^*_{PVDF}}{\Delta H^0_{PVDF}} \times 100 \qquad (4.1)$$

$$X_{BLEND(PVDF)}(\%) = \frac{\Delta H^*_{Blend}}{(0.8 \times \Delta H^0_{PVDF})} \times 100 \qquad (4.2)$$

$$X_{BLEND(PLA)}(\%) = \frac{\Delta H^*_{Blend}}{(0.2 \times \Delta H^0_{PLA})} \times 100 \qquad (4.3)$$

$$X_{TPV}(\%) = \frac{\Delta H^*_{TPV}}{(0.4 \times \Delta H^0_{PVDF}) + (0.1 \times \Delta H^0_{PLA})} \times 100 \qquad (4.4)$$

While, ΔH^* is the measured enthalpy of PVDF or PLA. ΔH^0 is the enthalpy of melting per gram of 100 % crystalline, 93 J/g for PLA (P. Boonfuang *et al.*, 2011) and 104.7 J/g for PVDF (Marega C. *et al.*, 2003). And percent crystallinity of the blends was calculated from the combination of the enthalpy of melting per gram of 100 % crystalline (ΔH^0) of PVDF and PLA.

The TPV blends were tested using MDR (rheoTECH MD+,Tech pro, A022S) under operation of 0.5 deg arc strain amplitude and rotor size L at various temperatures ranging from 180 – 200 °C.

4.3.6 Study of thermal properties of TPV blends after compression

Thermal properties of TPV samples after compression were characterized by using DSC (DSC822E model, Mettler Toledo) operated under nitrogen atmosphere with a flow rate of 10 ml/min. Every sample was heated from 30 °C to 200 °C with the heating rate of 10 °C/min and held for 3 minutes to delete a thermal history. Then, they were cooled down to 30 °C and re-heated again to 200 °C at the same rate. The second heating curves were reported. The cold crystallization temperature and melting temperature were obtained from second heating DSC thermograms. The relative percent crystallinity of PVDF and PVDF/PLA thermoplastic blends at the composition of 80PVDF/20PLA; X_{BLEND} (%) were calculated according to the equation 4.1, 4.2 and 4.3, respectively. TPV with 10 % of PLA and TPV without PLA at the rubber/thermoplastic composition on 50:50 ratio were calculated according to the equation 4.4 and 4.5, respectively. TPV with 10 % of PLA and TPV without PLA at the rubber/thermoplastic composition on 70:30 ratio were calculated according to the equation 4.6 and 4.7, respectively:

$$X_{PVDF}(\%) = \frac{\Delta H^*_{PVDF}}{\Delta H^0_{PVDF}} \times 100 \quad (4.1)$$

$$X_{BLEND(PVDF)}(\%) = \frac{\Delta H^*BLEND}{(0.8 \times \Delta H^\circ PVDF)} \times 100 \quad (4.2)$$

$$X_{BLEND(PLA)}(\%) = \frac{\Delta H^*BLEND}{(0.2 \times \Delta H^\circ PLA)} \times 100 \quad (4.3)$$

$$X_{TPV}(\%) = \frac{\Delta H^*_{TPV}}{(0.4 \times \Delta H^0_{PVDF}) + (0.1 \times \Delta H^0_{PLA})} \times 100 \quad (4.4)$$

$$X_{TPV}(\%) = \frac{\Delta H^*_{TPV}}{(0.5 \times \Delta H^0_{PVDF})} \times 100 \quad (4.5)$$

$$X_{TPV}(\%) = \frac{\Delta H^*_{TPV}}{(0.2 \times \Delta H^0_{PVDF}) + (0.1 \times \Delta H^0_{PLA})} \times 100 \quad (4.6)$$

$$X_{TPV}(\%) = \frac{\Delta H^*_{TPV}}{(0.3 \times \Delta H^0_{PVDF})} \times 100 \quad (4.7)$$

While, ΔH^* is the measured enthalpy of PVDF or PLA. ΔH^0 is the enthalpy of melting per gram of 100 % crystalline, 93 J/g for PLA (P. Boonfuang *et*

al., 2011) and 104.7 J/g for PVDF (Marega C. *et al.*, 2003). And percent crystallinity of the blends was calculated from the combination of the enthalpy of melting per gram of 100 % crystalline (ΔH^0) of PVDF and PLA.

4.3.7 Study of mechanical properties

The mechanical properties including the tensile strength, tear strength and hardness (shore A). Tensile test was done according to ASTM D412-06a or ISO 37 (type 1), tear test was done according to ASTM D624-00 or ISO 34 by using the universal testing machine (Instron, 4206-006 model) with load cell of 5 kN and crosshead speed of 500 mm/min. The hardness was determined according to ASTM D2240 by using shore A durometer (Zwick, type 7206). Five specimens were used in each case.

4.3.8 Study of thermal properties by using dynamic mechanical analyzer (DMA)

The storage modulus (E′), the loss modulus (E″), and the dissipation factor (tan δ) are measured by DMA (GABO-EPLEXOR 100N model) using a constant frequency of 1 Hz and a temperature range of -80°C to +120°C. The measurements were carried out under tension mode with a static load of 10 N and a dynamic load of 5 N. The dimensions of the test samples were in width*length*thickness (10*50*2 mm).

4.3.9 Study of oil swelling resistance properties

The oil resistance of the blends was studied after immersing sample in oil at temperature of 25 °C and 100 °C for 24 hours and 7 days according to ASTM D471-06 or ISO 2285 (Method A). In this study, gasohol 91, gasohol 95, E20 and E85 which contain 10, 10, 20 and 85 % ethanol, respectively, were used. After removal from the oil, the test pieces were wiped with tissue paper to remove excess oil from the surface and weighed immediately. The swelling index and percentage of swelling were calculated using equation 4.8 and 4.9, respectively:

$$Swelling\ index = \frac{Final\ mass}{Initial\ mass} \tag{4.8}$$

$$\%\ Swelling = \frac{Ws - Wo}{Wo} \times 10 \tag{4.9}$$

Where Ws refer to a swelling weight and Wo refer to an original weight.

4.3.10 Study of morphology

The morphology of rubber and plastic phases, the vulcanized rubber particles size and the dispersion of vulcanized rubber particles was examined by using the field emission scanning electron microscope (FE-SEM) HITACHI S-4800 model which contributed the images in the magnification range of 1,000 to 10,000 times at 10 kV. The samples must be coated with platinum under vacuum condition before observation to make them electrically conductive.

4.4 Results and discussion

4.4.1 Curing properties of ENR

Curing characteristics of ENR in DBPH system in terms of curing times, curing rates and torque values obtained from MDR were shown in table 4.3. Result from rubber compound needs shear force to distribute chemicals for vulcanization, MDR was used to investigate cure reactions. These results related to the finding of the suitable and practical temperature profile and screw speed in twin screw extruder because the excesses of curing temperature and curing times may result to exceed cross-linking reactions which cause the degradation of elastic properties, so the partially cured of ENR was needed to obtain after twin screw extruder and then fully cured in compression step.

As seen from table 4.3, the minimum elastic torque (S'@ML or ML) referred to extent of mastication, the lower ML higher extent of mastication during mixing. It can be seen that increase of DBPH resulted to lower extent of mastication. According to the maximum elastic torque (S'@MH or MH) was generally correlated with the stock modulus, the results showed that MH decreased as curing temperature

increased whereas it increased with DBPH contents due to higher extent of crosslinking. As curing temperature increasing, t_{90} was decreased whereas cure rate index (CRI) was increased due to the acceleration of crosslink reaction. CRI also was increased with DBPH contents but t_{90} insignificantly changed. Figure 4.1 clearly showed the effect of DBPH loading on MH and CRI.

The curing characteristics of ENR in DBPH system in terms of curing times and temperature at maximum curing reaction were investigated by using DSC in case of cure reaction occurred without any shear force to compare with the results from MDR. The results from DSC were shown in table 4.4 and 4.5.

As seen in table 4.4, the curing times decreased as curing temperature and DBPH contents increased. The results can be determined that at higher curing temperature and DBPH contents resulted to faster cure reaction which shown in lower curing times. Table 4.5 shown that around 188 – 190 °C are the best practical curing temperatures of ENR in DBPH system which shown the highest peak in figure 4.2 in all of DBPH contents.

Table 4.3 Cure characteristics of ENR at various DBPH content obtained from MDR

DBPH, phr	Upper and Lower die, °C	S'@ML, lbf·in	S'@MH, lbf·in	t_{90}, min	Cure rate index (CRI)
3	180	0.75	8.16	5.25	1.53
	190	0.79	7.36	2.16	3.59
	200	0.95	7.12	1.06	7.81
5	180	1.34	10.91	5.34	1.94
	190	1.30	10.24	2.26	4.71
	200	1.47	9.26	1.03	10.75
7	180	1.71	17.41	6.13	2.75
	190	1.81	15.89	2.17	7.94
	200	1.93	13.09	1.03	14.49

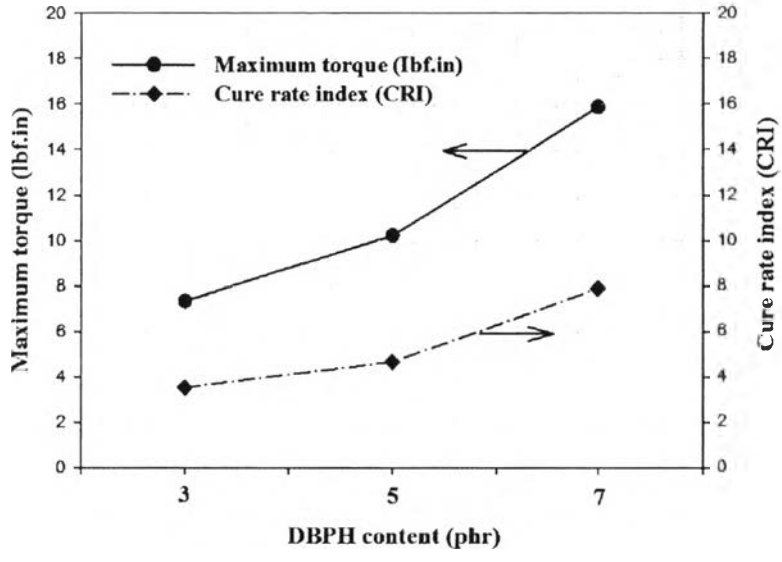

Figure 4.1 Maximum torque and cure rate index of the ENR compounds at various DBPH content (phr) obtained from MDR at 190 °C.

Table 4.4 Data of curing times of ENR at various temperature and DBPH contents obtained from DSC

Condition	Temperature, °C	DBPH, phr	Curing times, min
Isothermal method	180	3	12
		5	10
		7	6
Isothermal method	190	3	6
		5	5
		7	4
Isothermal method	200	3	3
		5	2.50
		7	2.25

It can be concluded that the temperature around 188 – 190 °C is the best working temperature of ENR in DBPH system which showed the highest curing

reaction. The faster curing reaction resulted from the increase of curing temperature and DBPH contents.

Table 4.5 Data of temperature at maximum curing reaction of ENR at various DBPH contents obtained from DSC

Condition	Temperature range, °C	DBPH, phr	Temperature at maximum curing reaction, °C
Non-isothermal method	30 - 300	3	190
		5	188
		7	190

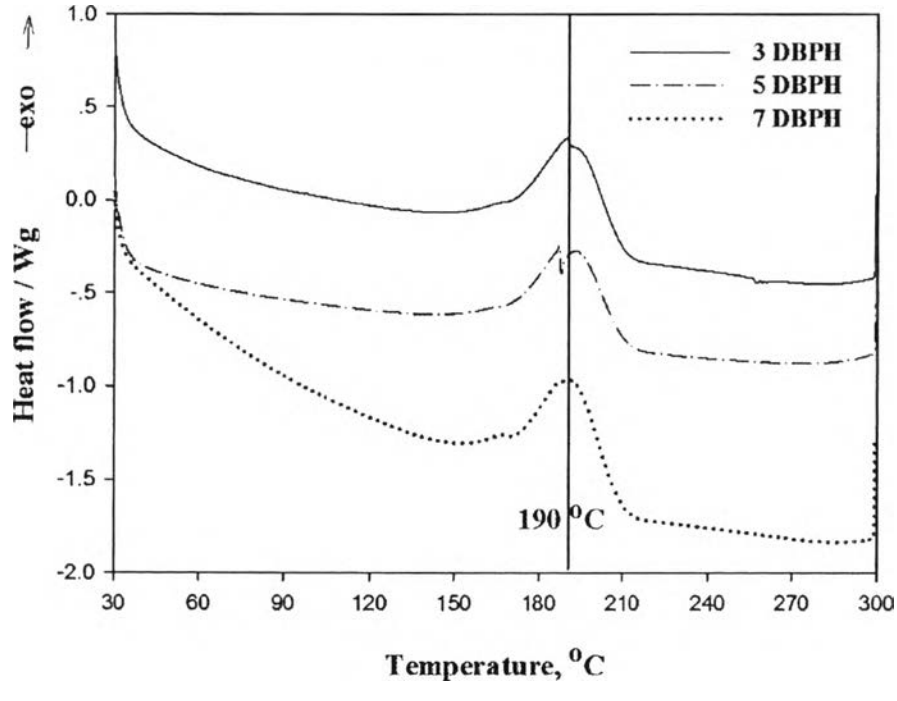

Figure 4.2 DSC thermograms showing curing curves of ENR at various DBPH contents.

4.4.2 Rheological properties

The rheological properties of ENR, PVDF, PVDF with triacetin, PVDF/PLA blends with triacetin were observed by using rheometer. The curves of relation between viscosity and shear rate at 180 °C and 190 °C were shown in figure 4.3 and 4.4, respectively. The viscosity curves of all materials at 180 °C and 190 °C are not different, significantly. The effect of adding PLA and triacetin could not pull down the viscosity of the blend in contrast to the higher temperature which resulted in lower viscosity. The table 4.6 showed the viscosity at shear rate 1200 (1/s) of the blends at 180, 185, 188 and 190 °C. These selected temperatures related to the heating zone in twin screw extruder. The results showed that during mixing of the blends in the screw, the viscosity of each phase was too close to each other as such morphology of the blends may be affected; i.e. phase inversion may not occur or uniform and fine dispersion of cured rubber phase may be difficult to successfully happen.

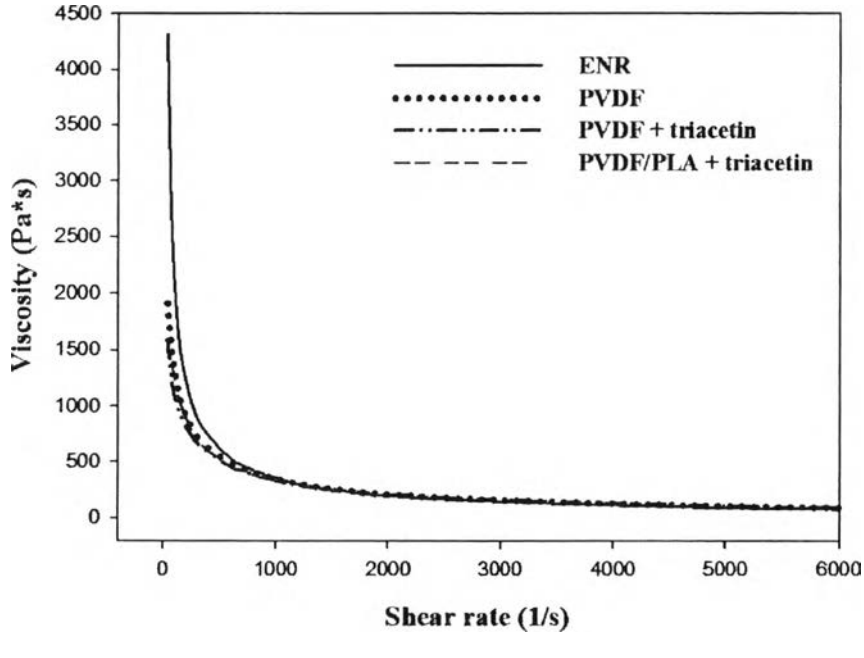

Figure 4.3 Viscosity as a function of shear rate at 180 °C.

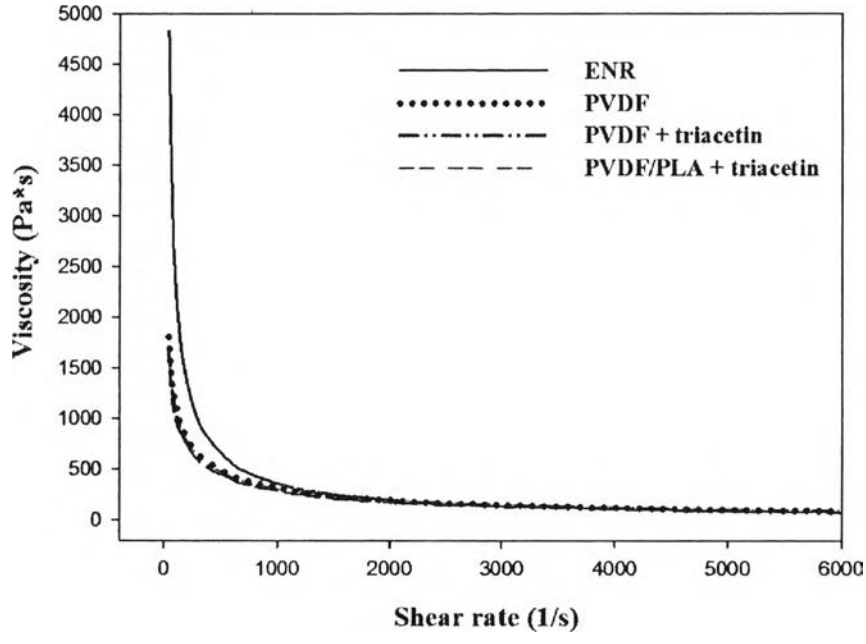

Figure 4.4 Viscosity as a function of shear rate at 190 °C.

Table 4.6 The viscosity (Pa*s) of ENR, PVDF, PVDF with triacetin and PVDF/PLA with triacetin at shear rate of 1200 (1/s)

Temperature (°C) / Materials	180	185	188	190
ENR	330	321	306	303
PVDF	308	298	288	282
PVDF + triacetin	295	275	254	250
PVDF/PLA + triacetin	288	278	250	244

4.4.3 Thermal properties of thermoplastic and TPV blends after twin screw extruder by using DSC

The DSC thermograms of PVDF, PLA and PVDF/PLA blends were shown in figures 4.5. Their thermal properties were shown in table 4.7. The glass

transition temperature (Tg) and melting temperature (Tm) of PLA appeared at 59 °C and 152.7 °C, respectively, close to the values reported in the literature of Hsin-Chieh Chen *et al.* [9]. Another cold crystalline peak of PLA located at 122 °C. There were two melting points of PLA in the PVDF/PLA blend located at 152.7 °C (β–form structure) and 145 °C (α-form structure). It can be seen that the crystallinity of PLA was decreased. Similarly, the crystallinity of PVDF decreased when adding PLA. Hsin-Chieh Chen *et al.* [9] revealed that the crystallinity of PLA decreased with an increasing PVDF contents which resulted in the immiscibility and Zhang *et al.* [10] also reported there was no favorable trend of PLA to form a miscible blend with PMMA because the crystallinity of PLA decreased with an increasing concentration of PMMA and some interaction between PLA and PMMA. Our results agreed with these reports.

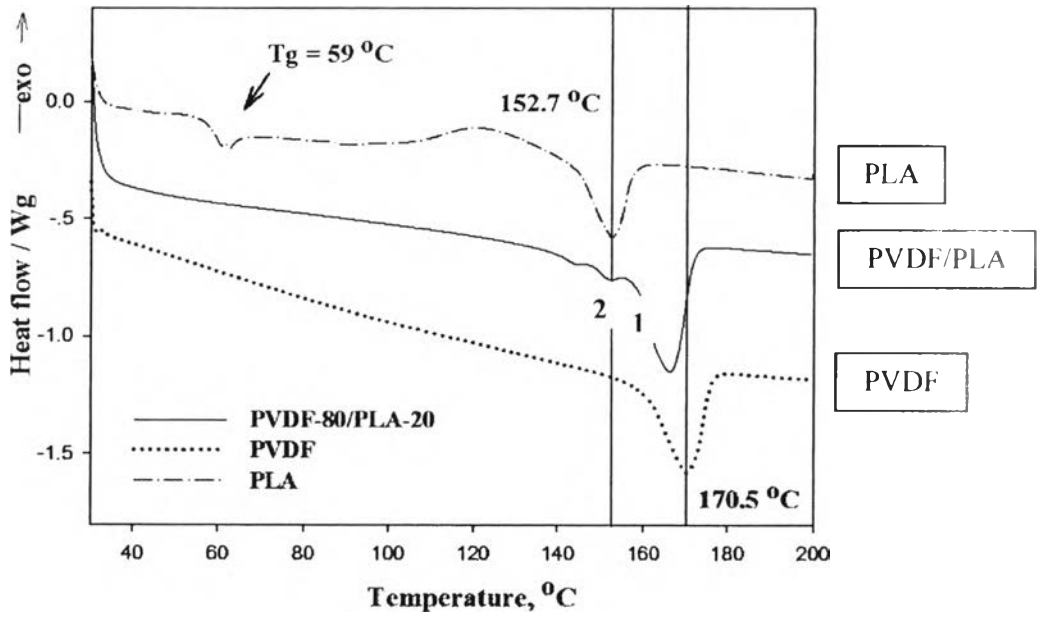

Figure 4.5 DSC thermograms showing heating curves of PVDF, PLA and PVDF/PLA blend.

Table 4.7 Melting temperature, crystallization temperature and percent crystallinity of PVDF and the blend

Materials	T_m (°C)	T_c (°C)	ΔH* (J/g)	Crystallinity (%)
PVDF	170.5	136.3	32.4	31
PLA	152.7	124.0	10.9	12
PVDF/PLA blend (PVDF)	166.2	134.5	24.3	29
PVDF/PLA blend (PLA 1)	151.7	-	0.67	3.6
PVDF/PLA blend (PLA 2)	143.7	-	0.27	1.4

The heating and cooling curves of TPV were compared with PVDF and PVDF/PLA blends in figure 4.6 and 4.7, respectively. Melting temperature, crystallization temperature and percentage of crystallinity of them were shown in table 4.8.

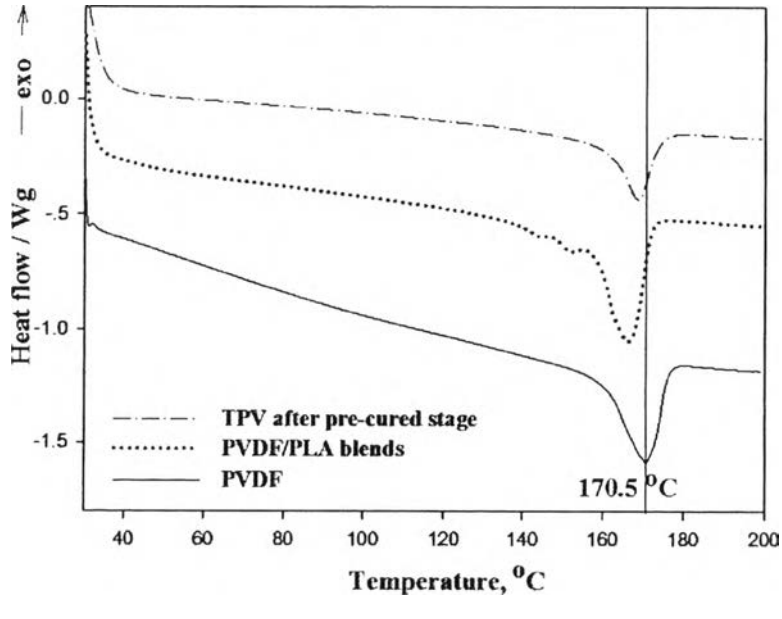

Figure 4.6 DSC thermograms showing heating curves of PVDF, PVDF/PLA blends and TPV after twin screw extruder.

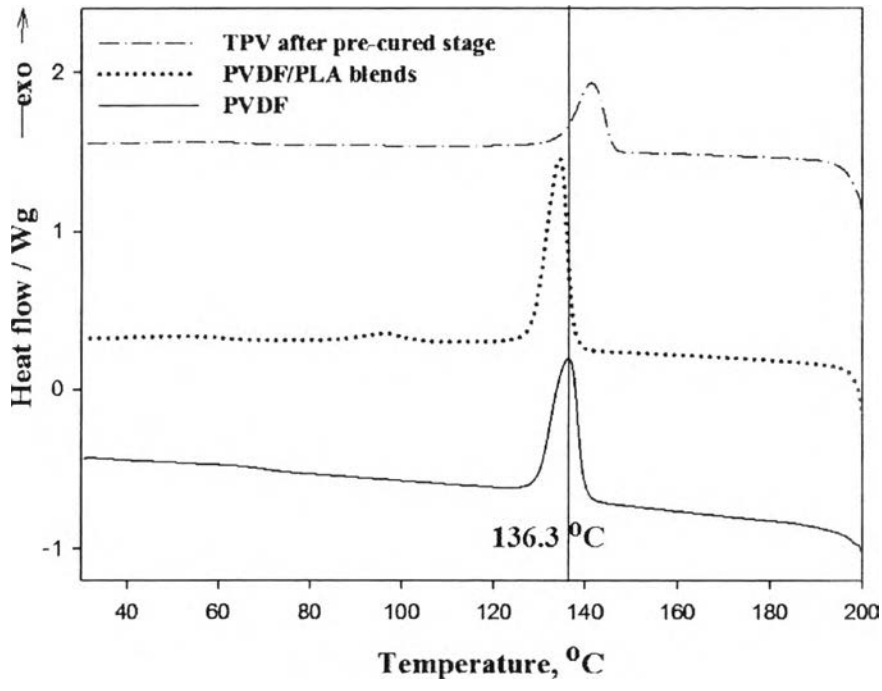

Figure 4.7 DSC thermograms showing cooling curves of PVDF, PVDF/PLA blends and TPV after twin screw extruder.

Table 4.8 Melting temperature, crystallization temperature and percent crystallinity of PVDF, PVDF/PLA blends and TPV

Materials	T_m (°C)	T_c (°C)	ΔH* (J/g)	Crystallinity (%)
PVDF	170.5	136.3	32.4	31
PVDF/PLA blends	166.2	134.5	24.3	29
TPV	168.6	141.5	18.9	36

From figure 4.6 and 4.7, TPV heating curve does not have any curing reaction which indicated as exothermic peak. So it can be concluded that TPV was fully cured in twin screw extruder. The nature of PLA is low crystallization, then cross-linking reaction tend to eclipse the crystallization of PLA which results to disappear of PLA position in both of heating and cooling curves of TPV.

4.4.4 Characteristics of TPV blends after twin screw extruder using MDR

The data of TPV obtained from MDR were shown in table 4.9. It can be seen that the minimum elastic torque (S'@ML or ML) increased with DBPH and ENR contents, whereas the addition of PLA and increase of curing temperature resulted to lower ML. Because the ML was related to process-ability, lower ML easier to process, therefore it can be concluded that addition of PLA and increase of temperature resulted in high process-ability. The maximum elastic torque (S'@MH or MH) increased with DBPH and ENR contents due to higher extent of crosslink, whereas the addition of PLA resulted to decrease in MH due to the low viscosity of PLA.

H. Ismail *et al.* [12] reported the lower the tan delta for a cured compound refers to the greater its resiliency. From the data, the tan delta @MH decreased with increasing ENR contents. The addition of PLA resulted to higher tan delta @MH which means lower resiliency of the compound. The maximum viscous torque (S"@MH) relates to the damping characteristics for a rubber compound. So it can be concluded that increase of DBPH and ENR contents resulted in higher damping characteristics.

Due to the fully cured after twin screw extruder which shown in DSC results (4.4.3), the well melt of thermoplastic parts and the non-degradation of rubber parts were needed to obtain after compression step. In this section, appearances were checked by eyes. The TPV samples obtained from MDR test were randomly checked by varying the curing times from 10 to 30 minutes depended on curing temperatures. The data were shown in table 4.10 and some samples were shown in figure 4.8. The results showed that the curing at 190 ^{o}C for 10 minutes gave a good appearance in all formula. Finally, compression conditions in terms of compression time and temperature were obtained.

Table 4.9 Data of during post-cured of TPV obtained from MDR

ENR/PVDF/ PLA, % wt	DBPH , phr	Upper and lower die temperature, °C	S'@ML , lbf·in	S'@MH , lbf·in	Tan delta @ MH	S''@MH , lbf·in
50/40/10	3	180	1.39	11.80	0.37	4.65
		190	1.06	11.37	0.42	4.35
		200	0.60	6.41	0.45	2.82
50/40/10	7	180	2.16	16.66	0.32	5.22
		190	1.15	15.24	0.43	6.12
		200	1.07	10.79	0.49	4.58
70/20/10	3	180	1.49	6.30	0.30	5.64
		190	1.39	6.37	0.22	4.49
		200	1.64	5.51	0.20	4.09
50/50/0	3	180	3.22	14.28	0.25	4.44
		190	2.70	10.30	0.24	4.05
		200	3.09	11.08	0.28	4.92
50/50/0	7	180	6.92	29.01	0.20	7.74
		190	6.14	21.18	0.21	6.66
		200	5.95	16.07	0.21	5.53
70/30/0	3	180	3.85	9.88	0.15	2.33
		190	3.34	8.75	0.12	2.55
		200	2.00	9.55	0.26	2.17

Table 4.10 Randomly checked an appearance of TPV after MDR

ENR/PVDF/ PLA, % wt	DBPH, phr	Upper and lower die temperature, °C					
		180		190		200	
		10 min	30 min	10 min	20 min	10 min	15 min
50/40/10	3	Δ	×	✓	×	✓	×
50/40/10	7	Δ	×	✓	×	✓	×
70/20/10	3	Δ	×	✓	×	×	×
60/40/0	3	Δ	×	✓	×	×	×
70/30/0	3	Δ	×	✓	×	×	×

✓ = Good appearance

Δ = Not good appearance; the plastic parts were not fully melted.

× = Not good appearance; the samples were broken or burned.

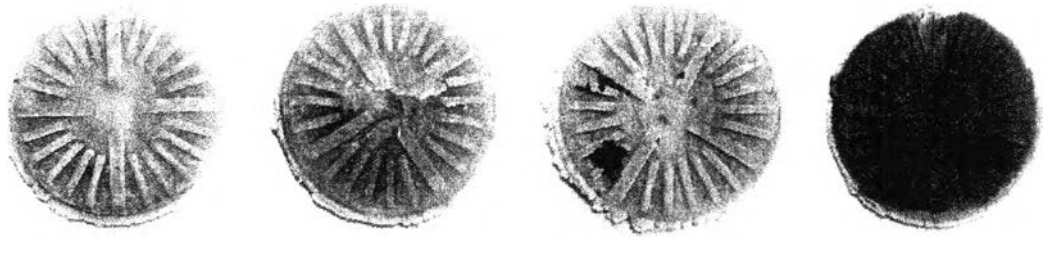

(A) (B) (C) (D)

Figure 4.8 The appearance of samples; (A) Good appearance, (B) Not good appearance with some cracked, (C) Not good appearance with some burned and (D) Not good appearance with all burned.

4.4.5 Thermal properties of TPV blends after compression

The DSC thermograms of TPV were observed by varying the ratio of ENR/PVDF/PLA and amount of DBPH. Materials formulas were shown in number code. For example, the ENR/PVDF/PLA (DBPH) ratio of 50/40/10 (3) mean 50 % of ENR, 40 % of PVDF, 10 % of PLA and 3 phr of DBPH. The result is shown in table 4.11 and DSC thermograms for all samples are shown in figures 4.9 – 4.10.

Table 4.11 The thermal properties of TPV at various ratio

Materials	Line	T_m of PVDF (^oC)	T_c of PVDF (^oC)	ΔH* of PVDF (J/g)	Crystallinity of PVDF (%)
PVDF/PLA blend	1	166.2	134.5	39.4	29
50/40/10 (0)	2	164.0	131.2	13.4	32
50/40/10 (3)	3	167.1	139.5	10.7	25.5
50/40/10 (7)	4	167.2	140.0	6.0	14.4
50/50/0 (3)	5	167.3	140.6	15.5	29.6
50/50/0 (7)	6	164.8	140.7	12.9	24.7
70/20/10 (3)	7	165.2	140.3	5.2	24.6
70/30/0 (3)	8	165.6	140.9	7.6	24

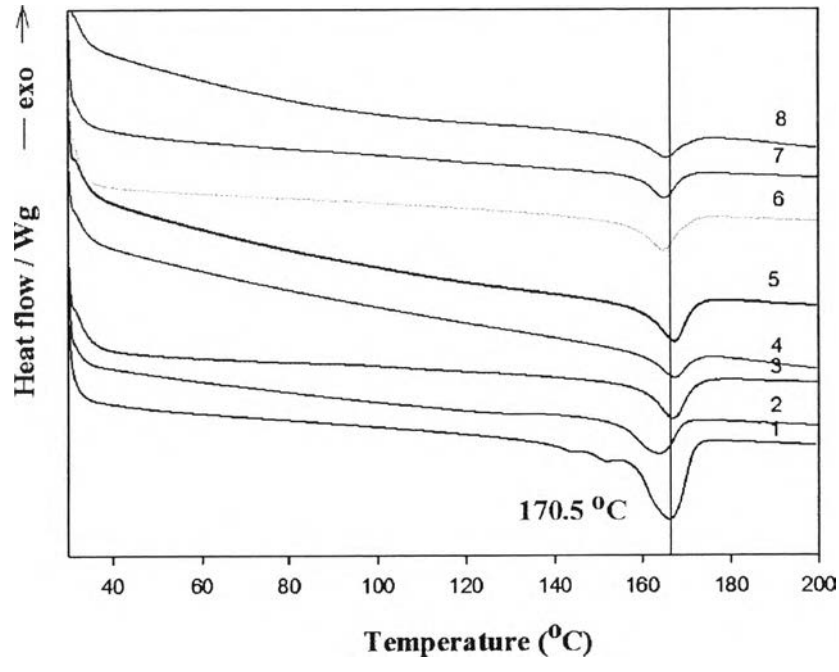

Figure 4.9 DSC thermograms showing heating curves of TPV at various ratio.

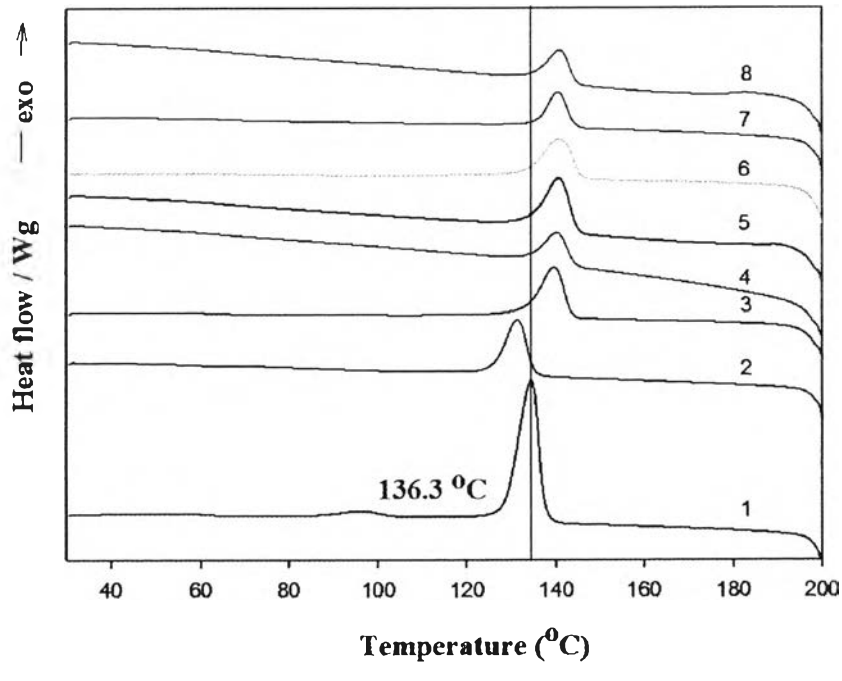

Figure 4.10 DSC thermograms showing cooling curves of TPV at various ratio.

From the results, added ENR into PVDF/PLA blend led to obstruct crystallization of PLA which didn't occurred PLA position in curves and smaller PVDF crystals sizes as well due to space limitation from cross-linking. At higher DBPH resulted to lower percent crystallinity due to higher extent of crosslinking. The percent crystallinity also decreased when added ENR into PVDF/PLA blend which can be indicated that ENR interrupted the crystallization and some grafting between ENR and thermoplastic blends was taken place. Beside, increased in melting temperature may resulted from crosslink reactions.

4.4.6 Mechanical properties

Mechanical properties in terms of tensile strength, Young's modulus at 0.2 % strain and percent elongation at break before aging were shown in table 4.12. There are 16 different formulations by varying contents of ENR, PVDF, PLA and DBPH. In addition, at DBPH 0 phr means ternary blends without vulcanization and ENR/PVDF/PLA of 100/0/0 means ENR system without adding thermoplastic.

The results showed that dynamic vulcanization significantly improved tensile strength and Young's modulus when compared to ternary blend and ENR system. The increase of DBPH in ENR system not much improved tensile strength. From figure 4.11, it is common to observe the increase in tensile strength with increasing thermoplastic content due to the increase in the rigidity of the blends. From figure 4.12, the tensile strength slightly increased with increasing DBPH. Moreover, if the degree of orientation of the molecular chains were hindered by the factors such as crosslinks, the tensile strength would drop, thereby the insignificant change of tensile strength at 7 phr reflected the high extent of crosslinking, Chantara Thevy Ratnam *et al.* [15] also suggested these observations.

According to the Young's modulus related to crosslink density, from figure 4.13, the Young's modulus increased as increase of thermoplastic and from figure 4.14, gradually increased with DBPH in vulcanized ENR/PVDF/PLA but showed steeply increased from 3 to 5 phr. The elongation at break gave results in contrast to tensile strength and Young's modulus. Z. Mohamad *et al.* [19] found that peroxide crosslink systems exhibit a brittle type fractured surface which resulted to decrease in elongation at break, our results also agreed with these observation.

Table 4.12 The tensile strength, Young's modulus at 0.2 % strain and percent elongation at break of the TPV blends before aging

ENR/PVDF/ PLA, % wt	DBPH, phr	Tensile strength, MPa	Young's modulus, MPa	Elongation at break, %
100/0/0	3	1.71 ± 0.20	2.08 ± 0.05	136.92 ± 8.74
	5	1.80 ± 0.07	2.94 ± 0.18	83.97 ± 9.03
	7	1.79 ± 0.14	4.19 ± 0.12	54.48 ± 3.97
50/40/10	0	2.45 ± 0.24	32.91 ± 5.89	35.64 ± 4.70
	3	4.67 ± 0.12	89.58 ± 5.71	36.65 ± 5.12
	5	5.08 ± 0.44	83.50 ± 3.17	38.13 ± 8.99
	7	6.02 ± 0.49	105.07 ± 7.96	33.59 ± 6.06
60/30/10	0	1.92 ± 0.37	25.59 ± 6.57	31.88 ± 5.77
	3	3.85 ± 0.63	72.53 ± 3.88	33.50 ± 5.87
70/20/10	0	1.40 ± 0.31	13.40 ± 3.94	92.92 ± 5.30
	3	2.54 ± 0.18	49.47 ± 6.43	33.93 ± 5.07
50/50/0	3	8.59 ± 0.30	131.94 ± 6.69	22.17 ± 1.93
	5	9.28 ± 0.39	250.36 ± 7.54	10.39 ± 1.59
	7	8.97 ± 0.62	226.38 ± 5.80	10.71 ± 1.43
60/40/0	3	5.98 ± 0.13	88.95 ± 8.20	24.07 ± 3.21
70/30/0	3	4.74 ± 0.11	56.68 ± 2.06	30.94 ± 7.43

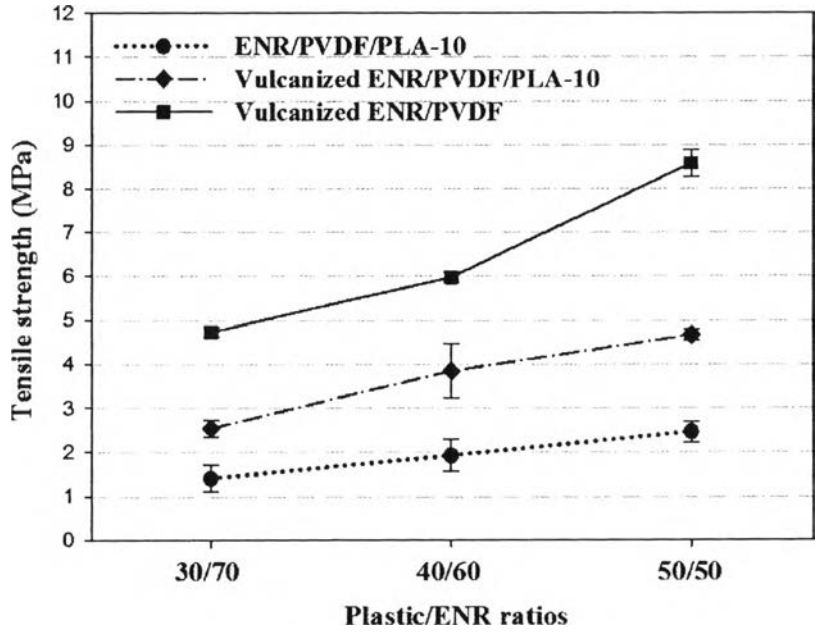

Figure 4.11 Tensile strength of ternary blend and TPV based on DBPH 3 phr using various plastic/ENR ratio.

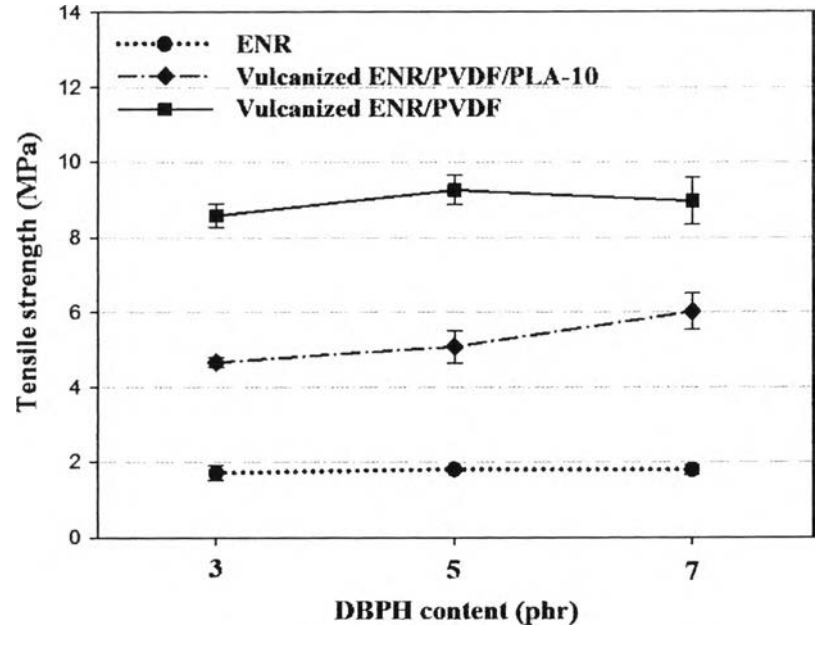

Figure 4.12 Tensile strength of ENR and TPV based on plastic/ENR at 50/50 using various DBPH contents.

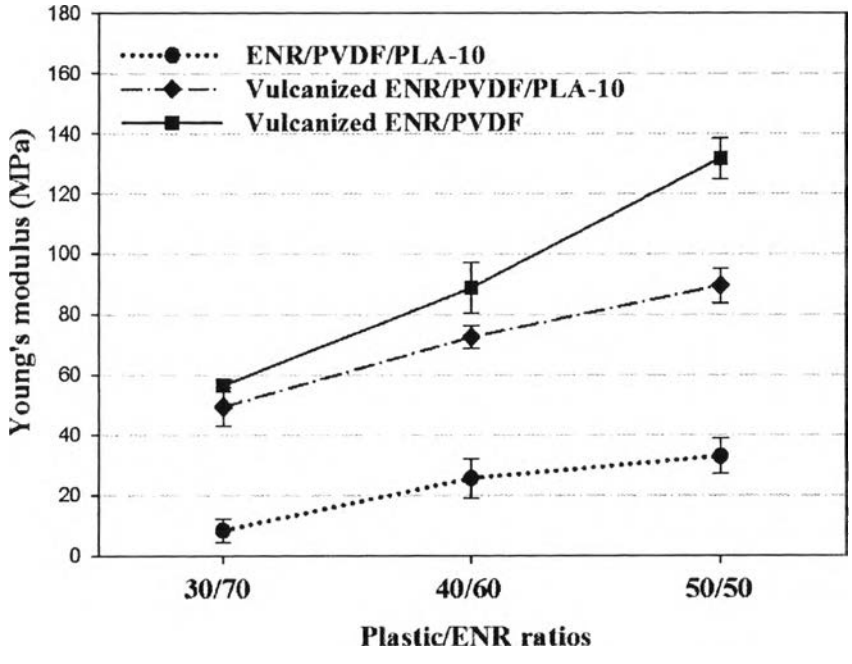

Figure 4.13 Young's modulus of ternary blend and TPV based on DBPH 3 phr using various plastic/ENR ratio.

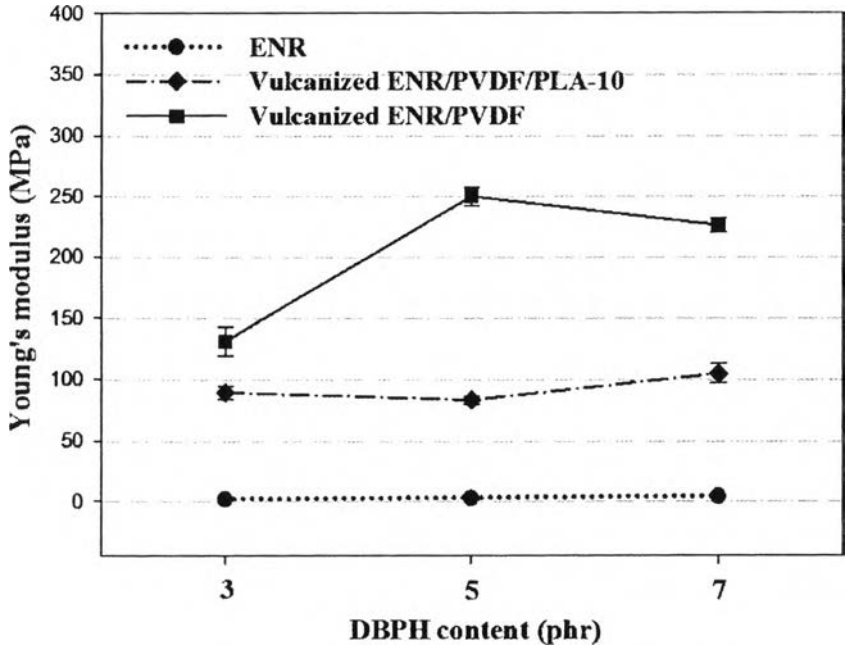

Figure 4.14 Young's modulus of ENR and TPV based on plastic/ENR at 50/50 using various DBPH contents.

Figure 4.15 showed the effect of plastic/ENR ratio and figure 4.16 showed the effect of DBPH content. When increasing DBPH, it undergoes crosslinking predominantly and starts losing its rubbery characteristics, which results in the progressive brittleness supported by the literature of Chantara Thevy Ratnam *et al.*[15], therefore the modulus increased while the elongation at break dropped with DBPH content.

Moreover, it can be concluded that the ENR/PVDF/PLA gave lower mechanical properties than ENR/PVDF due to embrittlement in thermoplastic blend phases and poor interfacial adhesion between PVDF and PLA which were supported by FE-SEM morphology in figure 4.17. These results effected to the low mechanical properties. Hsin-Chien Chen *et al.* [9] also reported the immiscibility blend between PVDF and PLA.

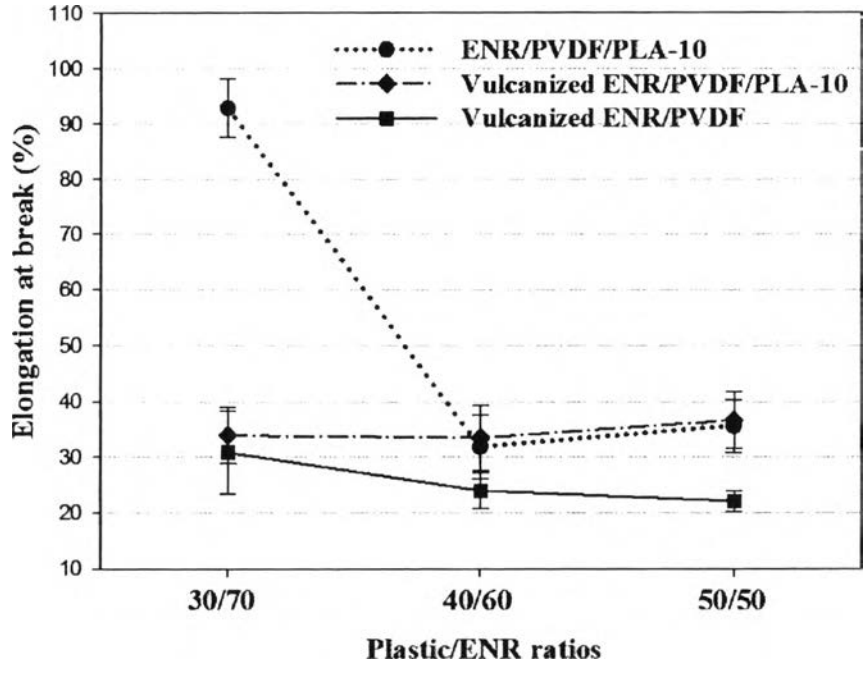

Figure 4.15 Elongation at break of ternary blend and TPV based on DBPH 3 phr using various plastic/ENR ratio.

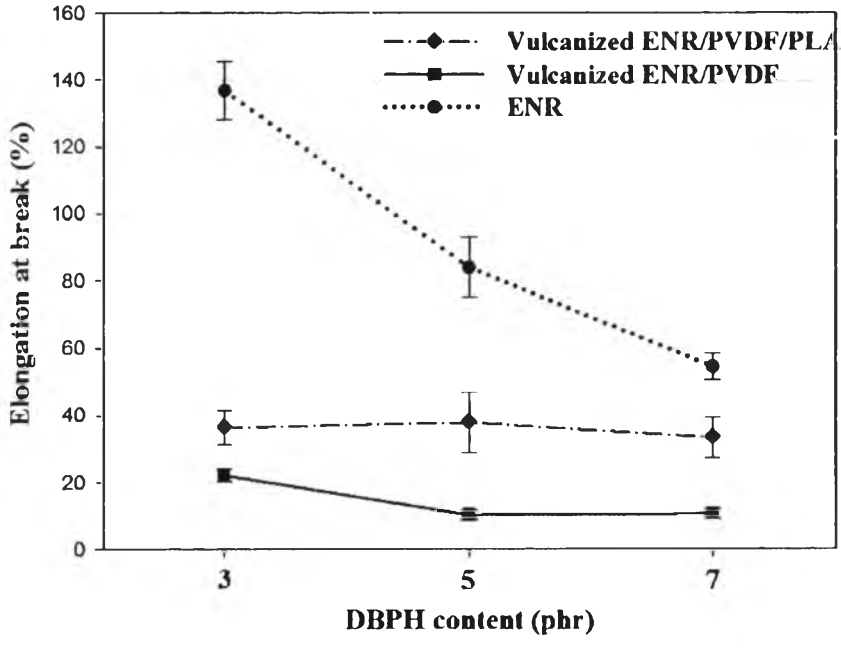

Figure 4.16 Elongation at break of ENR and TPV based on plastic/ENR at 50/50 using various DBPH contents.

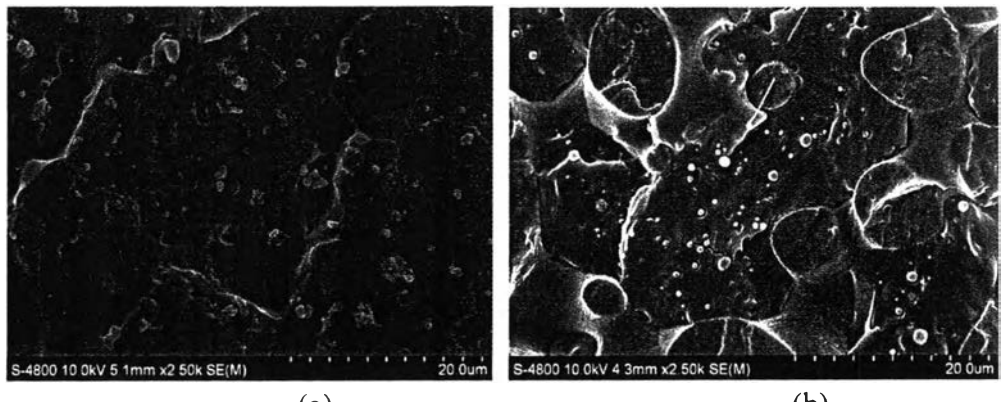

(a) (b)

Figure 4.17 The SEM morphology with 2500x magnification; (a) PVDF and (b) PVDF-80/PLA-20

Change in tensile strength, Young's modulus and elongation at break after thermal aging was shown in table 4.13, it seemed to be similar for all blends in terms of low properties due to the degradation of rubber phase in the presence of

peroxide, Z. Mohamad *et al.* also found the degradation of ENR phase in the presence of DCP at 2 phr.

Table 4.13 Changes in tensile strength, Young's modulus at 0.2 % strain and percent elongation at break of the TPV blends after aging

ENR/PVDF/ PLA, % wt	DBPH, phr	Tensile strength, MPa	Young's modulus, MPa	Elongation at break, %
100/0/0	3	-0.48	-0.46	-22.7
	5	-0.13	-0.31	+0.48
	7	-0.07	-0.44	+4.03
50/40/10	0	-0.58	-8.91	-6.46
	3	+0.09	-5.77	-18.6
	5	-0.29	-7.11	-22.0
	7	-1.05	-21.5	-16.8
60/30/10	0	-0.55	-7.74	+4.14
	3	-0.63	-17.2	-11.12
70/20/10	0	-0.63	-5.72	+115.7
	3	-0.58	-15.8	-15.7
50/50/0	3	+0.26	-0.57	-5.83
	5	+0.12	-87.3	+0.14
	7	-0.35	-95.9	-0.81
60/40/0	3	-0.36	-6.23	-11.3
70/30/0	3	-0.16	-5.92	-9.74

Tear strength and hardness both before and after thermal aging were shown in table 4.14 and 4.15, respectively. There are 16 different formulations by varying contents of ENR, PVDF, PLA and DBPH. As seen from figure 4.18 and

4.19, Tear strength gave similar trend with tensile strength. Hardness of ternary blend and ENR system showed significantly lower than that of TPV which were shown in figure 4.20 and 4.21. There was insignificant different in hardness between TPV adding PLA and non-adding PLA. It can be concluded that crosslinking affected slightly tear strength and hardness.

Table 4.14 The tear strength of the TPV blends

ENR/PVDF/ PLA, % wt	DBPH, phr	Tear strength, kN/m	
		Before aging	Change after aging
100/0/0	3	13.84 ± 3.66	-3.78
	5	10.16 ± 0.75	+0.92
	7	9.95 ± 0.60	+2.13
50/40/10	0	16.06 ± 1.73	+4.21
	3	37.84 ± 2.71	-10.0
	5	29.40 ± 2.35	-1.13
	7	31.92 ± 4.61	+0.85
60/30/10	0	13.86 ± 0.50	+1.67
	3	19.69 ± 2.69	-1.91
70/20/10	0	12.28 ± 0.84	+1.68
	3	16.95 ± 1.06	-6.09
50/50/0	3	63.00 ± 3.90	-0.58
	5	63.47 ± 3.98	+4.51
	7	61.18 ± 4.46	+6.71
60/40/0	3	42.58 ± 6.52	+2.33
70/30/0	3	35.94 ± 4.62	+1.27

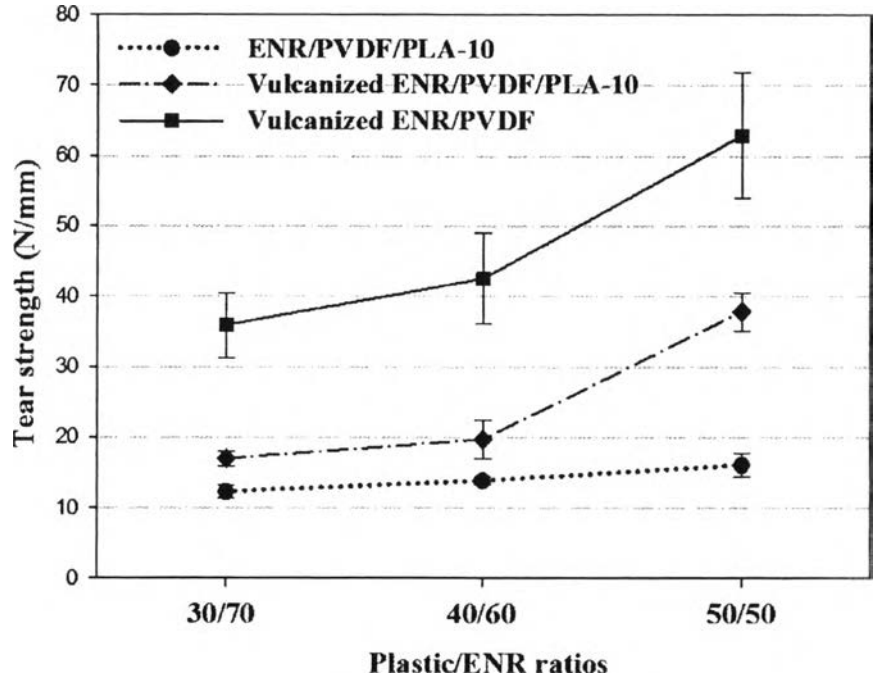

Figure 4.18 Tear strength of ternary blend and TPV based on DBPH 3 phr using various plastic/ENR ratio.

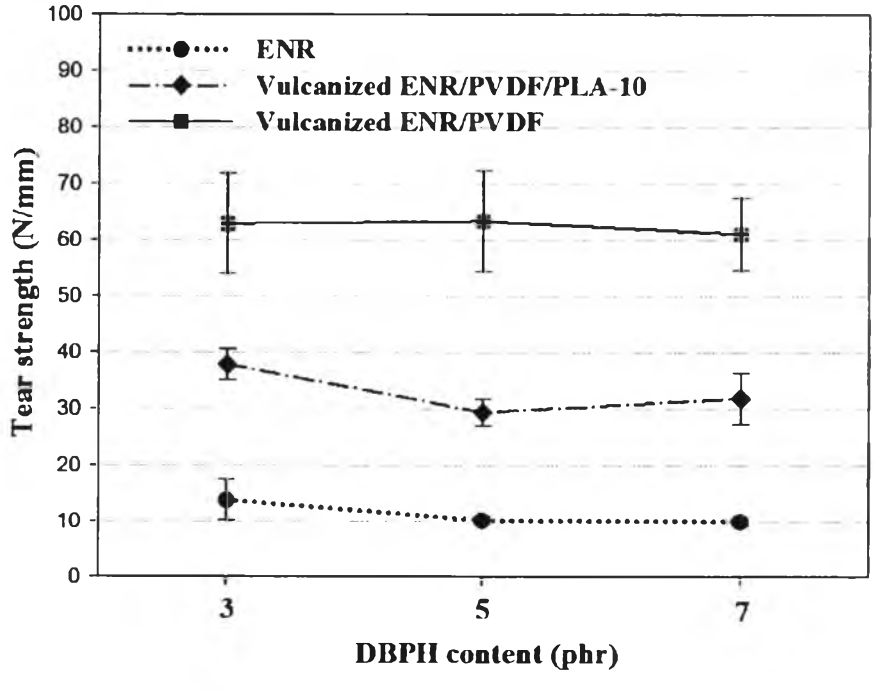

Figure 4.19 Tear strength of ENR and TPV based on plastic/ENR at 50/50 using various DBPH contents.

Table 4.15 The hardness of the TPV blends

ENR/PVDF/PLA, % wt	DBPH, phr	Hardness (Shore A)	
		Before aging	Change after aging
100/0/0	3	43.8 ± 1.30	-2.2
	5	46.4 ± 0.55	+3.0
	7	53.0 ± 0.00	+0.8
50/40/10	0	53.0 ± 3.53	+3.2
	3	65.2 ± 0.45	+1.2
	5	65.8 ± 1.30	+2.4
	7	65.6 ± 0.55	+4.4
60/30/10	0	53.2 ± 3.56	+5.4
	3	65.8 ± 1.09	+0.6
70/20/10	0	37.4 ± 4.93	-4.4
	3	64.2 ± 1.64	+1.2
50/50/0	3	64.4 ± 1.67	+1.8
	5	65.2 ± 1.64	+1.6
	7	65.6 ± 1.67	+3.8
60/40/0	3	64.6 ± 1.52	+2.8
70/30/0	3	64.4 ± 1.52	+1.4

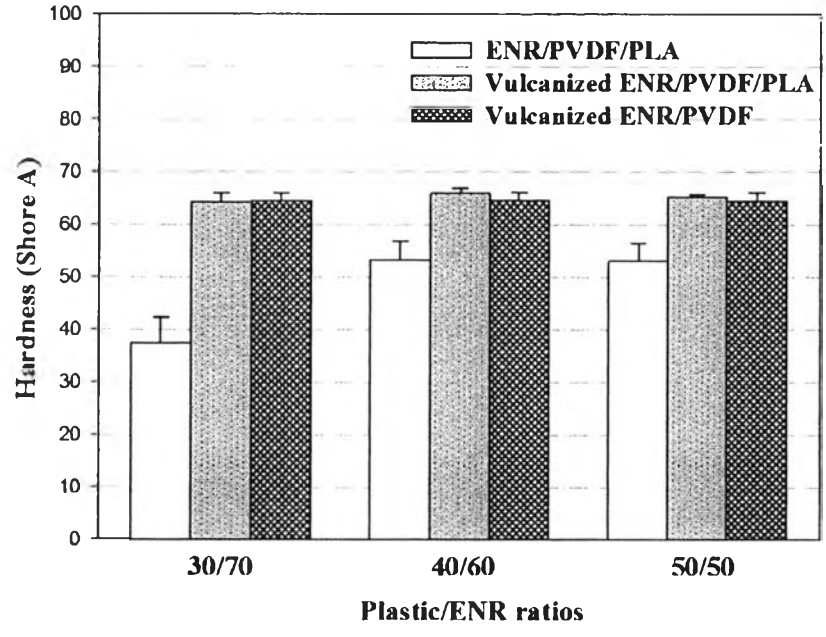

Figure 4.20 Hardness of ternary blend and TPV based on DBPH 3 phr using various plastic/ENR ratio.

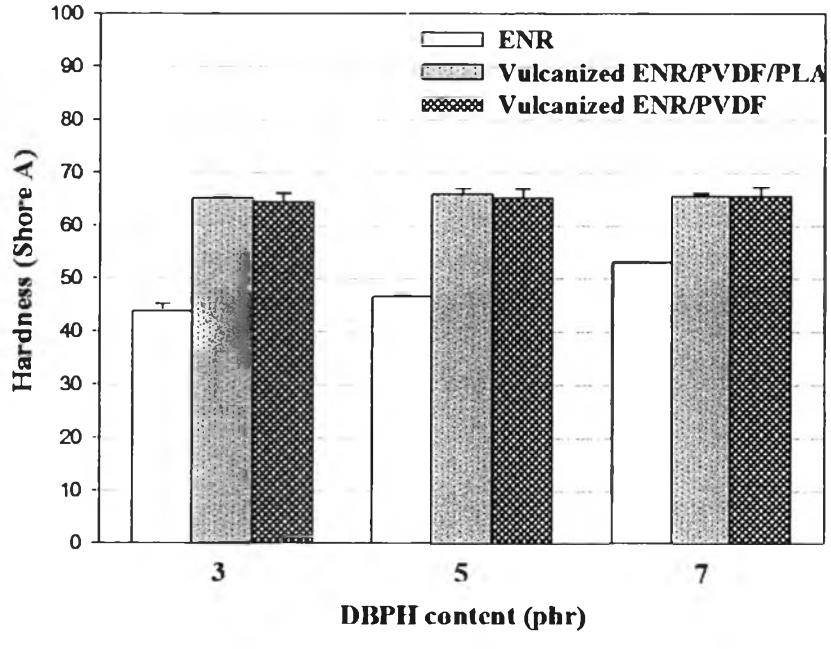

Figure 4.21 Hardness of ENR and TPV based on plastic/ENR at 50/50 using various DBPH contents.

4.4.7 Dynamic mechanical properties

Figure 4.22 and 4.23 represented the temperature dependence of storage modulus (E') and loss factor (tan delta), respectively on the effects of dynamic vulcanization, ENR/plastic ratios and addition of PLA. The explanations of the sample name were shown here, for example, ENR 3 means ENR-cured system using DBPH at 3 phr, Ternary blend 50:50 means the ternary blend system between ENR/PVDF/PLA at the ENR/plastic ratio of 50/50 and 70303_NO PLA means the TPV system without PLA at ENR/plastic/DBPH ratio of 70/30/3.

The effects of TPV and dynamic vulcanization showed significant increase in storage modulus compared to ENR-cured and ternary blend systems. The storage modulus of TPV with PLA was lower than TPV without PLA at the lower temperature region (below 0°C). This may be attributed to incorporate of PLA that formed some cracks and voids between PVDF and PLA phases due to the immiscibility, which may be responsible for decreased in the storage modulus. At 20 – 40 °C, the TPV of 50/50 ENR/plastic ratio showed higher storage modulus than the others which related to the Young's modulus results.

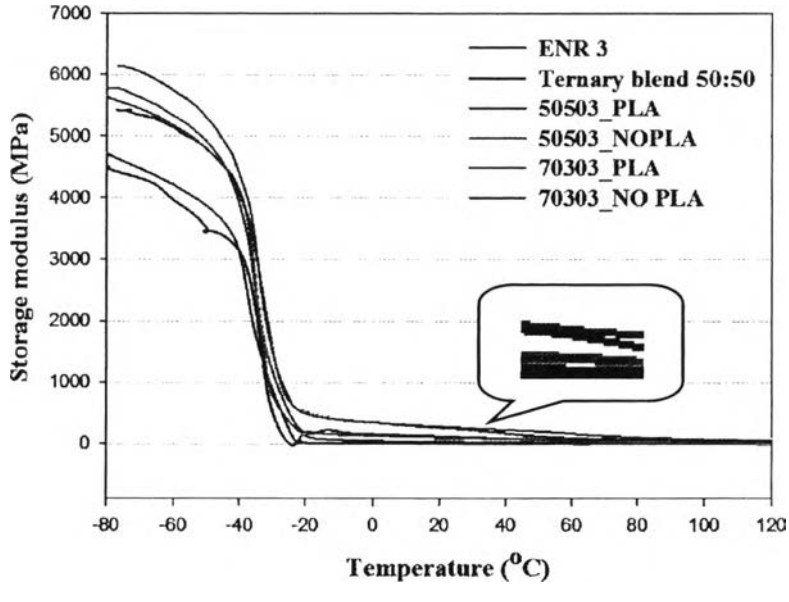

Figure 4.22 Effects of dynamic vulcanization, ENR/plastic ratios and addition of PLA on the storage modulus as a function of temperature.

As seen from figure 4.23, the tan delta curve of ENR-cured at DBPH 3 phr showed a peak at -25 °C which corresponded to the glass transition temperature (Tg). The incorporation of thermoplastic contents both of ternary blend and dynamically vulcanized blend showed significant decrease in tan delta peak compared to ENR-cured system. This corresponded to reinforcing tendency of the thermoplastic materials. R. Rajasekar *et al.* [5] reported the reduction of chain mobility owing to physical and chemical adsorption of the rubber molecules caused a height reduction of tan delta peak during dynamic mechanical deformation. The decrease in tan delta peak proved minimum heat buildup related to lower damping characteristics. Snooppy George *et al.* [7] revealed that the PP/NBR blends on peroxide vulcanization that there was a possibility of degradation of the PP phase in the presence of peroxide which related to the lowest loss modulus compared to other cured-systems.

Moreover, the dynamic mechanical investigation was used to predict the miscibility of the system. The TPV with PLA blends showed two tan delta peak around -28 and +50 °C, which corresponded to the Tg of ENR and PLA, respectively. Two clearly separated peaks indicated that the ENR and PLA phases were not fully compatible. The obtained glass transition temperature of ENR is at -25 °C. The Tg of PVDF is at -35 °C reported by R. D. Simoes *et al.* [18]. There was a single tan delta peak in between the Tg of these two components but it can't be concluded that the ENR and PVDF phases were miscible because the Tg of them were close (< 20 °C), miscibility can't be judged from Tg measurements. SEM morphology studies can help to indicate the miscibility by observing the phase separation and interfacial adhesion.

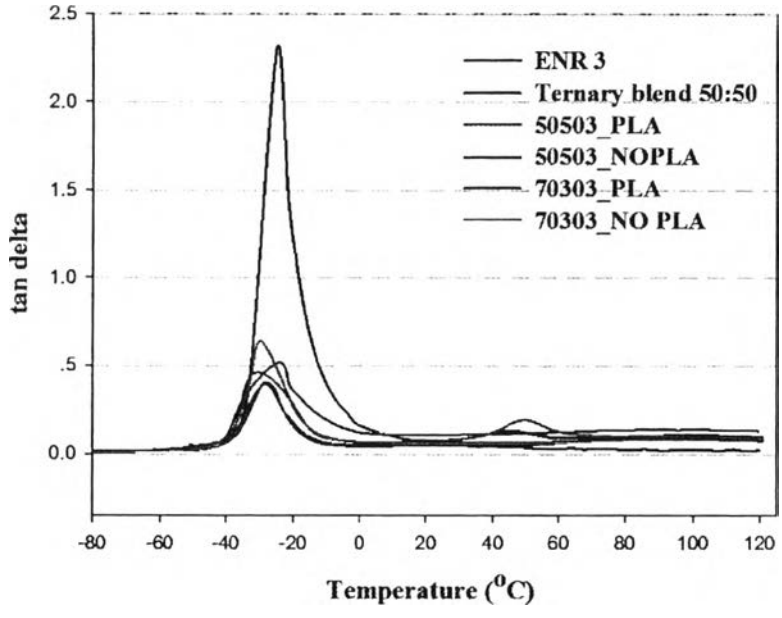

Figure 4.23 Effects of the dynamic vulcanization, ENR/plastic ratios and addition of PLA on the tan delta as a function of temperature.

Figure 4.24 and 4.25 represented the temperature dependence of storage modulus (E') and loss factor (tan delta), respectively on the effects of DBPH contents and addition of PLA. The increase of DBPH showed significant increase in storage modulus due to the extent of crosslinking and TPV with PLA showed lower storage modulus than that of without PLA which were discussed above. At 20 – 40 ^{o}C, all blends gave similar storage modulus values which related to the insignificant change of Young's modulus with increasing DBPH contents.

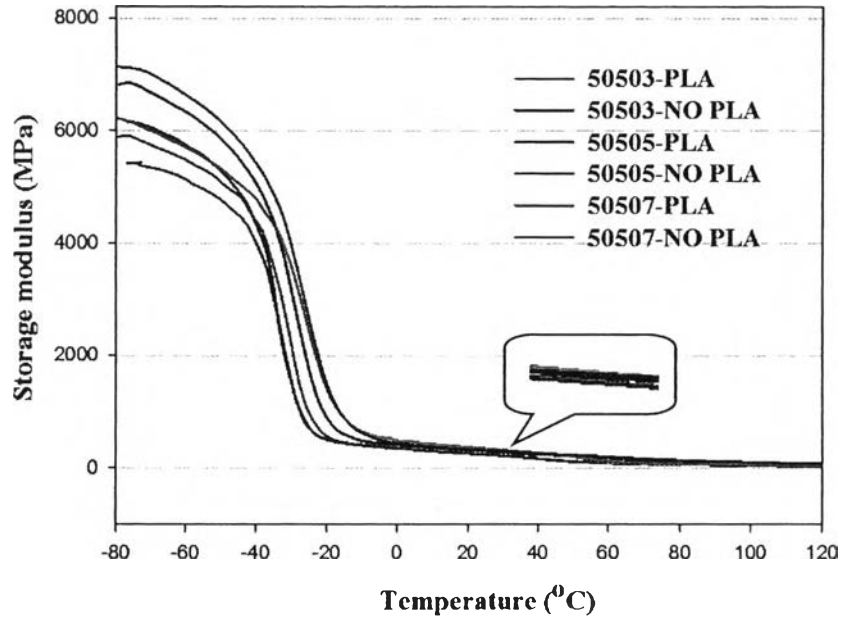

Figure 4.24 Effects of the DBPH contents and addition of PLA on the storage modulus as a function of temperature.

As seen from figure 4.25, the tan delta peak decreased with increasing DBPH which attributed to the increase of glass transition temperature. This can be explained by the reason of increasing in overall crosslink density that resulted to a greater restriction of the molecular mobility for a given temperature. The area under tan delta peak reported the damping characteristics which decreased with increasing DBPH contents. Liao *et al.* [8] suggested that the damping characteristics of the dynamically cured blend depended on the blend composition and the curative level, our work also agreed with these observations. The Tg of PLA in 50507-PLA system was shifted to a higher temperature which attributed to the restriction of the PLA molecular chain mobility. This may be due to the introduction of crosslink structure into PLA which stiffen the PLA. Sen-lin Yang *et al.* [13] found that the PLA could be crosslinked by adding small amounts of crosslinking agent triallyl isocyanurate (TAIC) and DCP, these observations supported our discussion above.

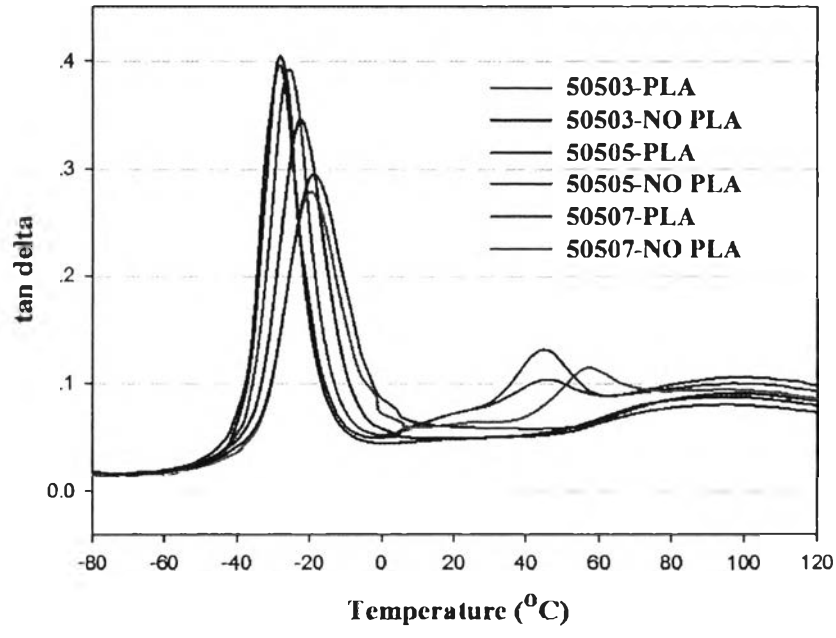

Figure 4.25 Effects of the DBPH contents and addition of PLA on the tan delta as a function of temperature.

4.4.8 Oil swelling properties

Oil swelling test was done in gasohol 91, gasohol 95, E20 and E85 at room temperature and 100 °C for 24 hours and 7 days. Figure 4.26 – 4.29 studied the effects of the dynamic vulcanization, ENR/thermoplastic ratios and addition of PLA on the oil resistance in 4 oil types including effects of higher temperature and longer time of immersion. The explanations of the sample name were shown here, for example, 5050-Ternary blend means the ternary blend system between ENR/PVDF/PLA at the ENR/plastic ratio of 50/50, 6040-PLA means the PLA added TPV system at ENR/plastic ratio of 60/40 and 7030-NO PLA means the TPV system without PLA at ENR/plastic ratio of 70/30.

According to the oil swelling resistance related to the extent of crosslinking, it were revealed that the dynamic vulcanization significantly improved the oil resistance and decreased the rate of oil uptake which showed in terms of TPV gave lower swelling index than ternary blend and TPV insignificantly changed the swelling after immersed for 7 days. It can be concluded that as higher ENR contents resulted to higher oil swelling due to lower crosslink density, the adding of PLA not

clearly affected the oil swelling properties in TPV system and as higher percent ethanol in oil resulted to lower oil swelling index.

Due to no crosslink in ternary blend system, it could not be tested at high temperature of 100 °C because the shape of samples was fully damaged. So the results only showed the swelling index of TPV systems. Focusing on the same period of immersion, the higher temperature increased the oil swelling, especially in ENR/plastic ratio of 70/30, whereas the ratios of 50/50 and 60/40 showed slightly increased in oil swelling. After immersed the samples at 100 °C for 7 days, the results showed the quite similar swelling index in ENR/plastic ratios of 50/50 and 60/40 both of adding and non-adding PLA, whereas the ratio of 70/30 clearly increased the swelling index.

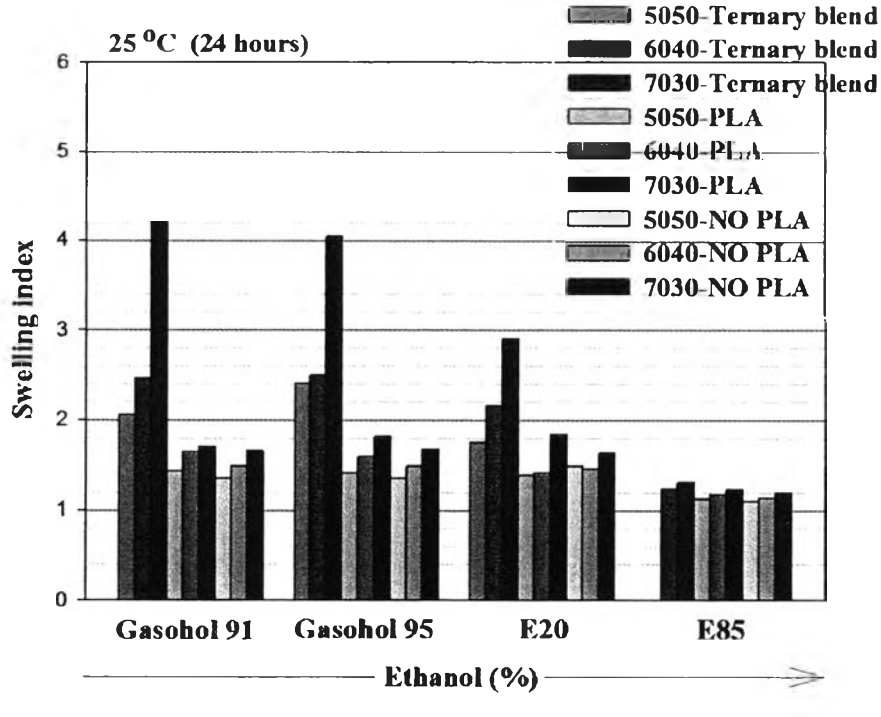

Figure 4.26 Oil swelling index using DBPH at 3 phr by varying the ENR/plastic ratios at room temperature for 24 hours.

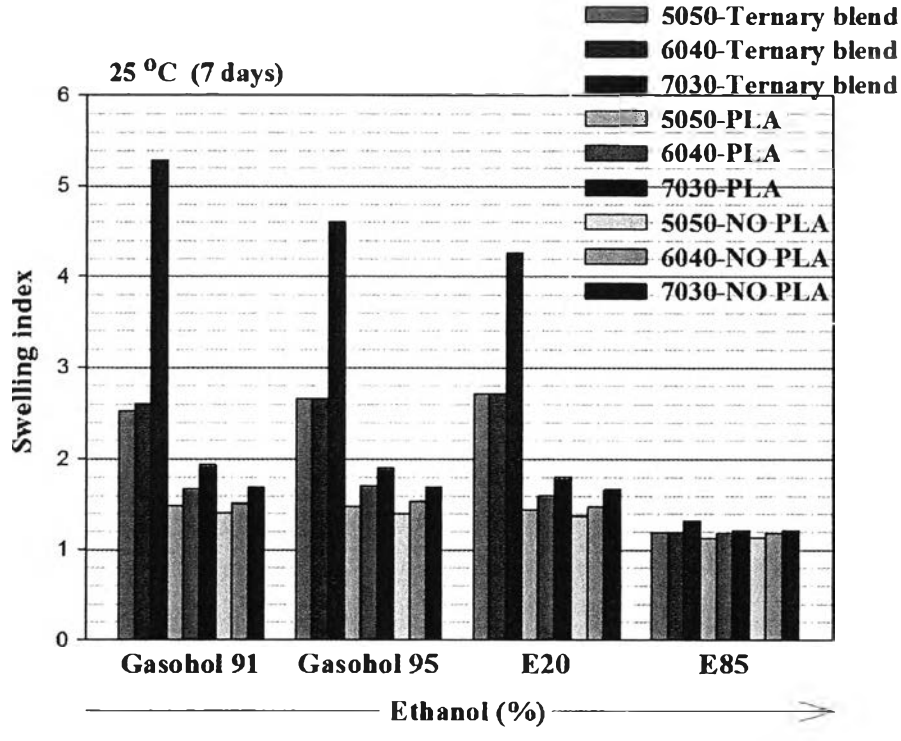

Figure 4.27 Oil swelling index using DBPH at 3 phr by varying the ENR/plastic ratios at room temperature for 7 days.

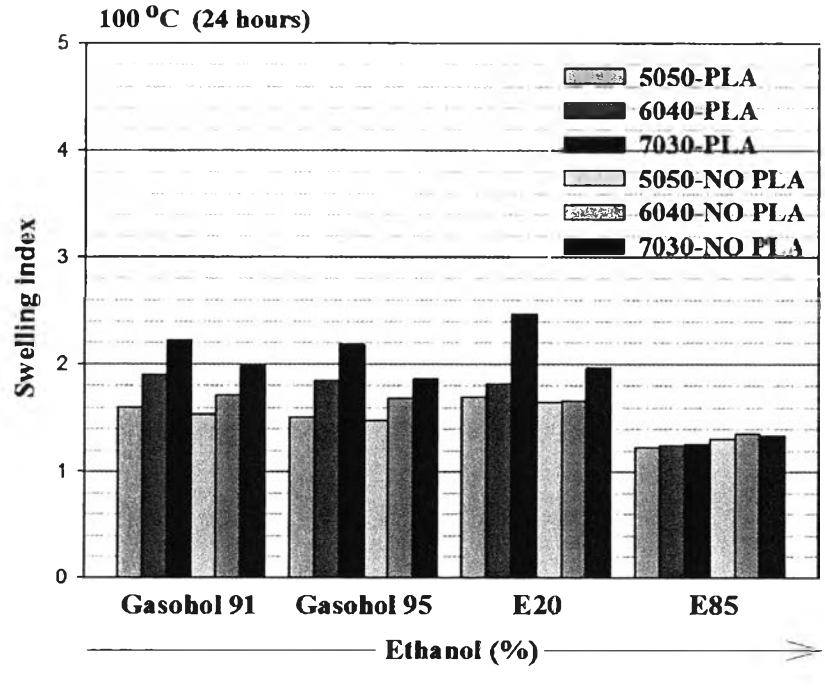

Figure 4.28 Oil swelling index using DBPH at 3 phr by varying the ENR/plastic ratios at 100 °C for 24 hours.

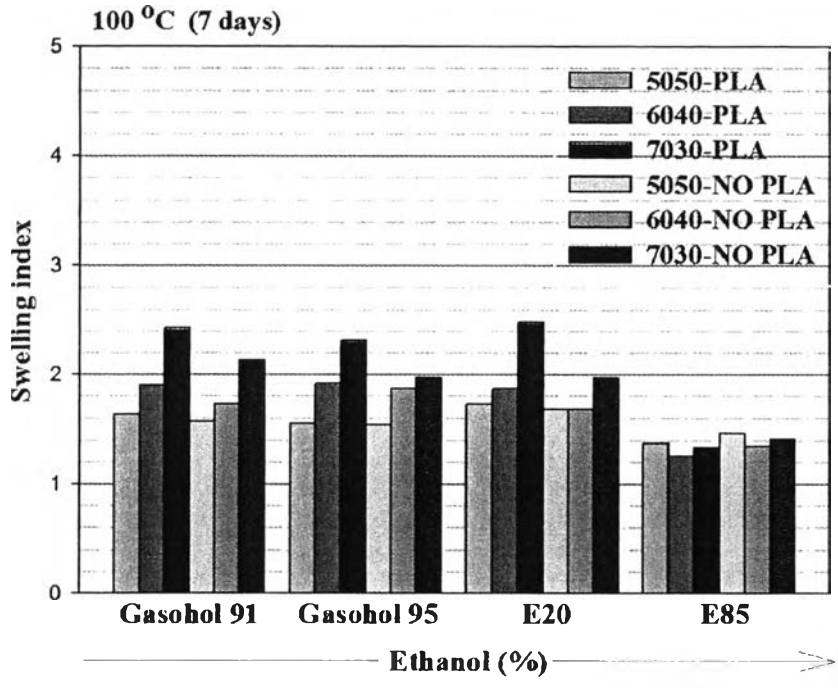

Figure 4.29 Oil swelling index using DBPH at 3 phr by varying the ENR/plastic ratios at 100 °C for 7 days.

Next, the oil swelling index focused on the effect of TPV comparing to rubber-cured system, contents of DBPH and addition of PLA. Figure 4.30 – 4.33 showed the swelling results at each condition. The explanations of the sample name were shown here, for example, ENR 3 means the ENR-cured system using DBPH 3 phr, 50505-PLA means the PLA added TPV system using DBPH 5 phr and ENR/plastic ratio of 50/50 and 50507-NO PLA means the TPV system without PLA using DBPH 7 phr and ENR/plastic ratio of 50/50.

According to content of DBPH and presence of TPV resulted to higher oil resistance, it can be seen that the TPV systems significantly improved the oil resistance when compared to ENR-cured systems and also decreased the rate of oil uptake after immersion for 7 days. The increase of DBPH over 3 phr gave significant decrease in oil swelling due to higher crosslink density, whereas the DBPH at 7 phr insignificantly improved the oil resistance from using DBPH at 5 phr which attributed to the maximum of crosslink density that could occurred. The addition of PLA insignificantly affected the swelling properties.

Focusing on the same period of immersion, the higher temperature effected to higher swelling index, especially in the composition of DBPH 3 phr. The swelling index of TPV at DBPH 5 and 7 phr gave similar trend in all of oil types. The increase of DBPH content only affected the oil resistance in ENR-cured systems which insignificantly affected in TPV system. After immersed the sample in oil at 100 °C for 7 days, the swelling index of ENR-cured system increased, whereas that of TPV systems gave quite similar results as the 24 hours immersion. Finally, it can be concluded that the presence of TPV clearly improved the oil swelling resistance and also heat resistance.

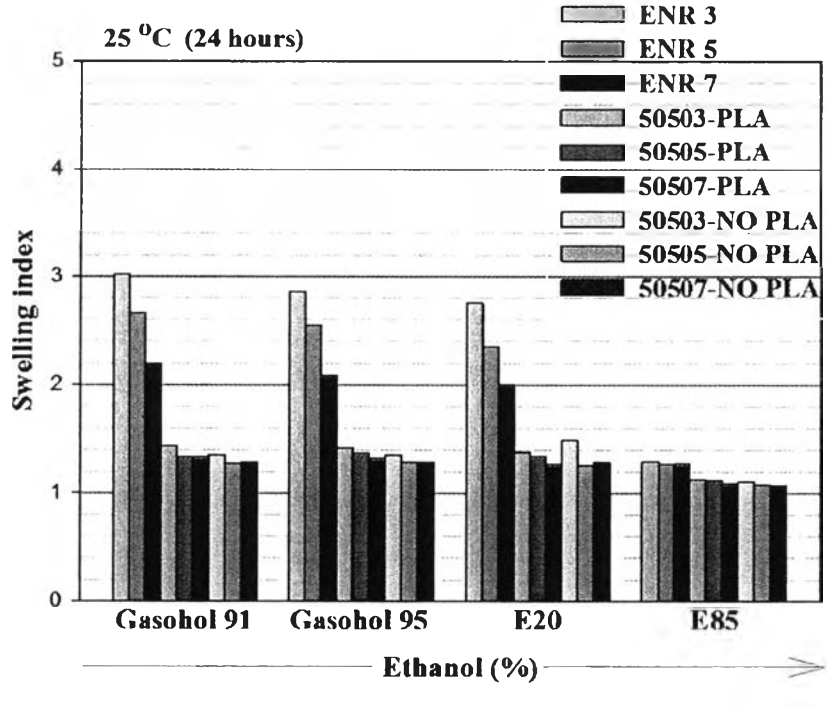

Figure 4.30 Oil swelling index at fixed ENR/plastic ratio of 50/50 by varying the DBPH contents at room temperature for 24 hours.

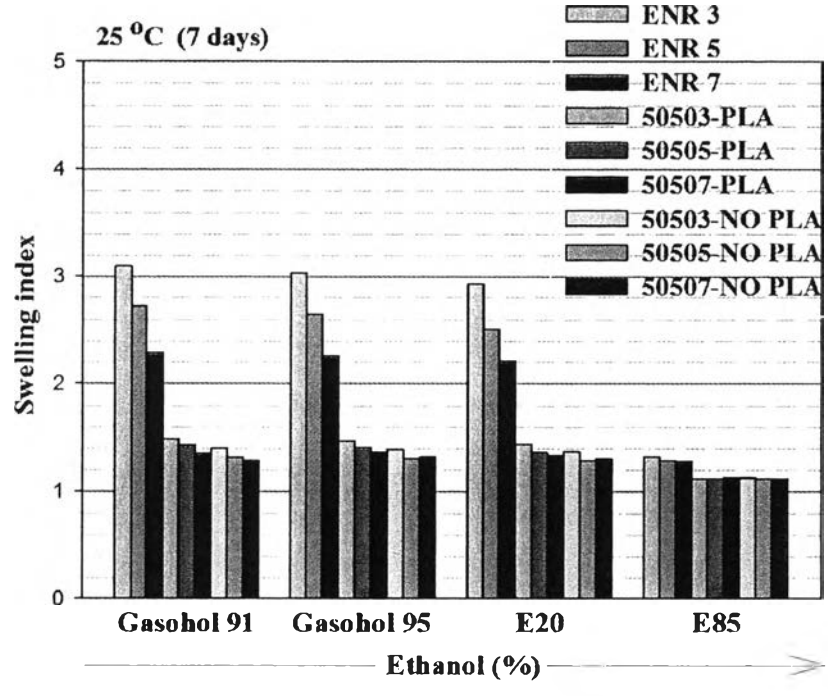

Figure 4.31 Oil swelling index at fixed ENR/plastic ratio of 50/50 by varying the DBPH contents at room temperature for 7 days.

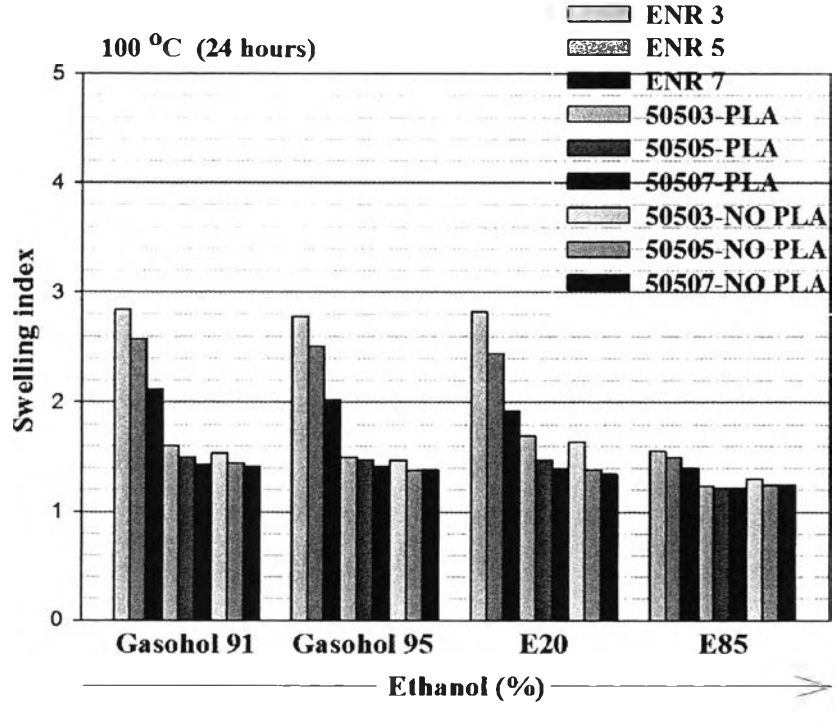

Figure 4.32 Oil swelling index at fixed ENR/plastic ratio of 50/50 by varying the DBPH contents at 100 °C for 24 hours.

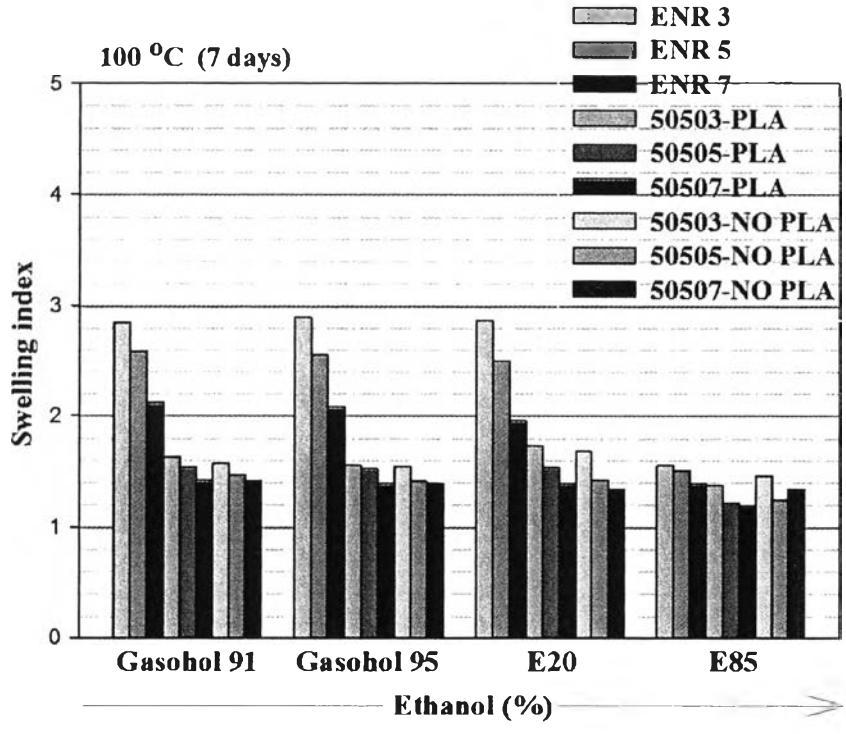

Figure 4.33 Oil swelling index at fixed ENR/plastic ratio of 50/50 by varying the DBPH contents at 100 °C for 7 days.

The appearance of TPV after oil immersion at room temperature (25 °C) for 24 hours was shown in figure 4.34. Focusing on the original samples before immersing, the ENR/thermoplastic ratio of 50/50 (figure 4.34 (a) and (b)) showed the white spots on the surface of samples which belonged to the thermoplastic phases but the ratio of 70/30 (figure 4.34 (c) and (d)) only showed tiny white spots because the main component is ENR phase. The increase of gasoline contents significantly affected to the surface appearance in all the blends, especially for the ratio of 70/30 due to the high contents of ENR, whereas immersion in E85 (containing 15 % gasoline and 85 % ethanol) insignificantly affected to the surface appearance.

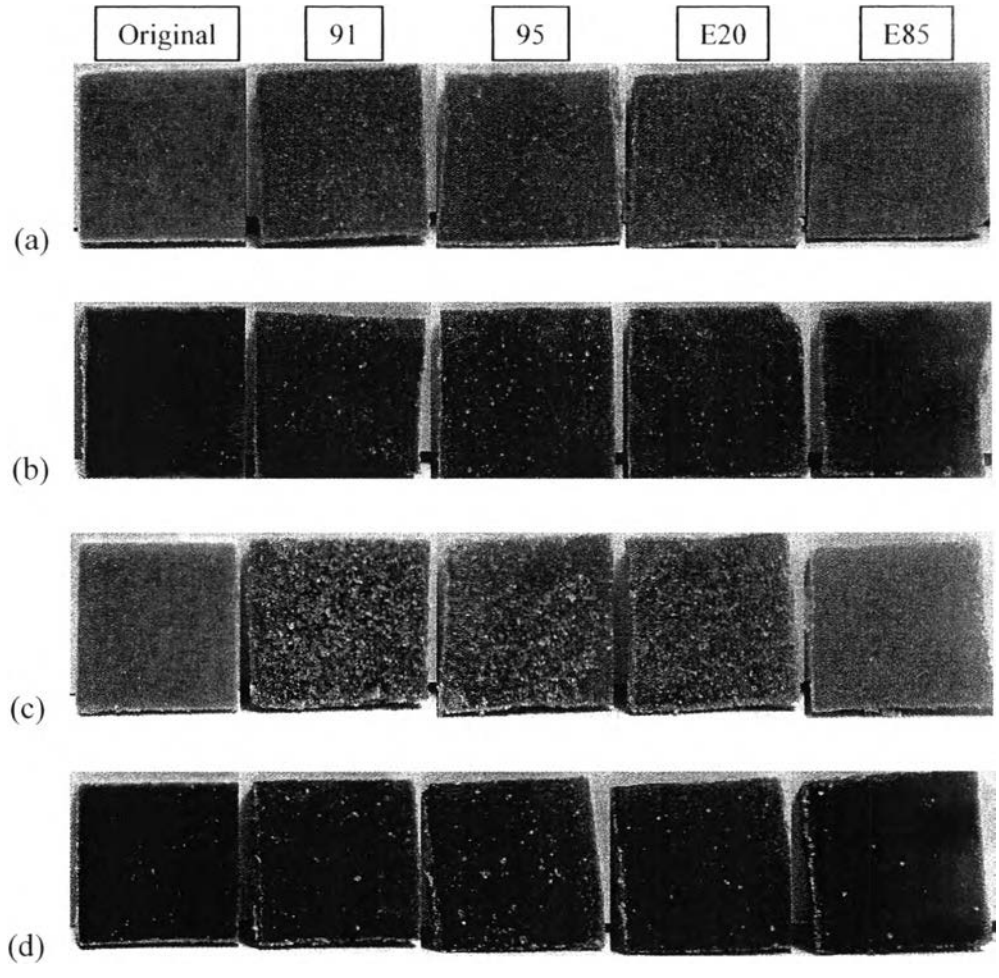

Figure 4.34 Immersed samples in different oil types which were original sample, gasohol 91, gasohol 95, E20 and E85 from left to right, respectively. The immersion was done at 25 °C for 24 hours: (a) 50505-PLA, (b) 50505-NO PLA, (c) 70303-PLA and (d) 70303-NO PLA.

4.4.9 SEM Morphology

SEM images recorded by scanning the samples along the cross section of fractured surface provided further details of the morphology of the blends. They revealed that the morphology observed at the cross section was similar to that found at the volume of the blends, which is important information.

Focusing on the thermoplastic phases, the SEM morphology revealed that the PVDF-80/PLA-20 blend in figure 4.17 (b) showed the poor interfacial adhesion in terms of some voids and cracks between PVDF and PLA phases. These effects resulted to the less of mechanical properties.

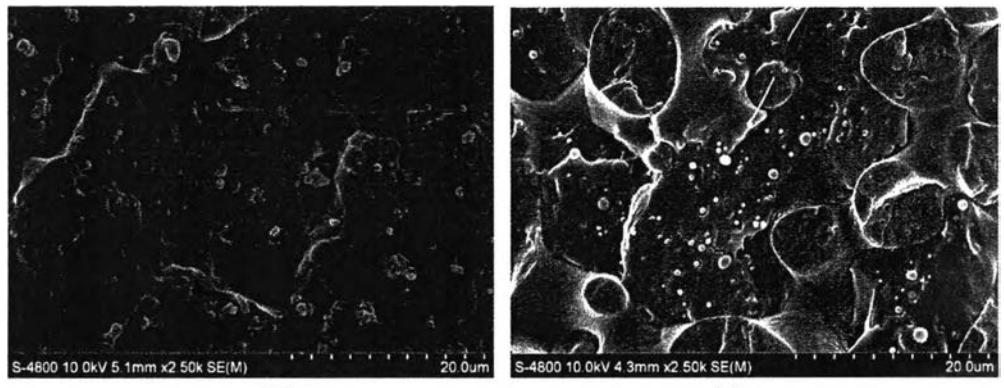

(a) (b)

Figure 4.17 The SEM morphology with 2500x magnification; (a) PVDF and (b) PVDF-80/PLA-20

Figure 4.35 revealed the studies of SEM morphology of TPV blends. The explanation of samples code name were shown here, for example, 50505-PLA means the ENR/thermoplastic/DBPH ratio of 50/50/5 with adding PLA. According to the literature of R.D. Simoes *et al.* [18], the rougher region was PVDF phase while the smoother region was ENR phase. It can be seen that the ENR phase coalesced brought to the coalescence of ENR domain, especially in the ratio of 50/50 which showed the co-continuous phase and large size of ENR and thermoplastic domain while the ratio of 70/30 showed smaller size of rougher region of thermoplastic domain that attributed to the main phase belong to ENR. Comparing between figures 4.35 (B) and (C), the size characteristic of thermoplastic domain was similar but the figure (B) showed some voids due to the effect of adding PLA which also can be seen in figure (A). This may attributed to poor interfacial adhesion between PLA and other components. Focusing on the interfacial adhesion between ENR and PVDF phases, it revealed that these two components had good interfacial adhesion due to no appearance of cracks and voids at the domain edges.

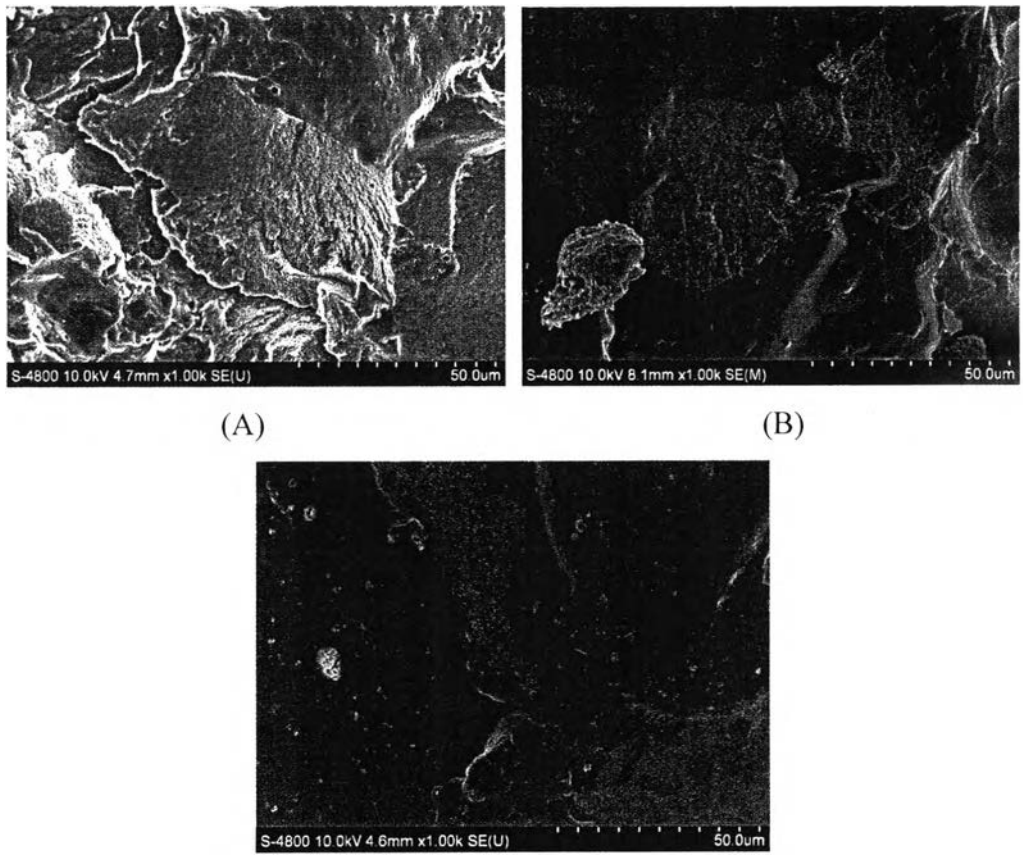

Figure 4.35 The SEM morphology with 1000x magnification; (A) 50505- PLA, (B) 70303-PLA and (C) 70303-NO PLA.

4.5 Conclusion

The effects of thermoplastic, DBPH and PLA contents including the dynamic vulcanization on cure characteristics, rheological, mechanical, oil resistant and morphological properties have been studied. The results showed that the increase of DBPH in the ENR compounds gave higher cure rate index and maximum torque. The viscosity of thermoplastic and rubber phases was nearly same and the addition of PLA and triacetin insufficiently decreased the viscosity in thermoplastic phase. The ENR/PVDF gave better mechanical properties in terms of tensile and tear strength, Young's modulus and hardness including oil resistance than ENR/PVDF/PLA, especially the ENR/PVDF/DBPH blend ratio of 50/50/5. The SEM morphology

revealed that the PVDF/PLA blend was immiscible which showed some voids and cracks at the interface, these results were supported by the two tan delta peak obtained from DMA. The phase morphology of the ENR/plastic ratio of 50/50 revealed the co-continuous form.

4.6 Acknowledgements

This work was granted by National Research Council of Thailand (NRCT), The Petroleum and Petrochemical College, Chulalongkorn University and National Center of Excellence for Petroleum, Petrochemicals and Advanced Materials.

4.7 References

1. Supri and H. Ismail (2006). Effects of dynamic vulcanization and glycidyl methacrylate on properties of recycled poly(vinyl chloride)/acrylonitrile butadiene rubber blends. *Polymer Testing*, 25, 318-326.
2. Yamoun C. and Magaraphan R. Peroxide Cured NaturalRubber/Fluoroelastomer/High Density Polyethylene via Dynamic Vulcanization.
3. Phothiphon K. (2010). Functionalized natural rubber: rubber parts for gasohol resistance. *A thesis submitted in partial fulfillment of the requirements for the degree of master of science, PPC. Chulalongkorn University.*
4. P. Boonfaung, P. Wasutchanon and A. Somwangthanaroj (2011). Development of packaging film from bioplastic polylactic acid (PLA) with plasticizers. *PACCON2011 (Pure andapplied chemistry international conference).*
5. R. Rajasekar, Kaushik Pal, Gert Heinrich, Amit Das and C.K. Das (2009). Development of nitrile butadiene rubber - nanoclay composites with epoxidized natural rubber as compatibilizer. *Materials and design*, 30, 3839 – 3845.

6. Das A, Costa FR, Wagenknecht U, Heinrich G (2008). Nanocomposites based on chloroprene rubber: effect of chemical nature and organic modification of nanoclay on the vulcanizate properties. *Eur Polym J*, 44, 3456 – 65.
7. Snooppy George, N.R. Neelakantan, K.T. Varughese and Sabu Thomas (1997). Dynamic mechanical properties of isotactic polypropylene/nitrile rubber blends: effects of blend ratio, reactive compatibilization and dynamic vulcanization. *Journal of polymer science: Part B: Polymer physics*, 35, 2309 – 2327.
8. F. S. Liao, A. C. Su and Tzu – Chien J. Hsu (1994). *Polymer*, 35, 2579.
9. Hsin – Chieh Chen, Chen – Hao Tsai and Ming – Chien Yang (2011). Mechanical properties and biocompatibility of electrospun polylactide/poly(vinylidene fluorides) mats. *J Polym Res*, 18, 319 – 327.
10. Zhang G, Zhang J, Wang S and Shen D (2003). *J Polym Sci Polym Phys*, 41, 23.
11. Li. Y and Shimizu H. (2007). *Macromol Biosci*, 7, 921.
12. H. Ismail and R. Ramli (2007). Organoclay filled natural rubber nanocomposites: The effects of filler loading and mixing method. *Journal of reinforced plastics and composites*, 27, 16 – 17.
13. Sen – lin Yang, Zhi – Hua Wu, Wei Yang and Ming – Bo Yang (2008). Thermal and mechanical properties of chemical crosslinked polylactide (PLA). *Polymer testing*, 27, 957 – 963.
14. A. J. Nijienhuis, D. W. Grijpma and A. J. Pennings (1996). *Polymer*, 37, 2783.
15. Chantara Thevy Ratnam and Mohd Saiful Ahmad (2006). Stress – Strain, morphological and rheological properties of radiation – crosslinked PVC/ENR blend. *Malaysian Polymer Journal*, 1, 1 – 10.
16. Lyons, B. J. (1993). The effect of radiation on the physical and chemical properties of polyethylene containing and antioxidant and /or other additives. *Radiation Physical Chemistry*, 42, 197 – 205.
17. Nelisen L. E. (1962). *Mechanical properties of polymers*. Van Nostrand Reinhold Company, New York.

18. R. D. Simoes, A. E. Job, D. L. Chinaglia, V. Zucolotto, J. C. Camargo – Filho, N. Alves, J. A. Giacometti, O. N. Oliveira Jr and C. J. L. Constantino (2005). Structural characterization of blends containing both PVDF and natural rubber latex. *Journal of Raman spectroscopy,* 36, 1118 – 1124.

19. Z. Mohamad, H. Ismail and R. Chantara Thevy. Tensile properties and morphology of dynamically vulcanized ENR-50/EVA blends: Different vulcanization system. *Journal of chemical and natural resources engineering,* 91 - 98.